

DIGITAL SIMULATION OF TWELVE PULSE CONVERTER

A Thesis Submitted
In Partial Fulfilment of the Requirements
for the Degree of
MASTER OF TECHNOLOGY

By

SUBROTO BHATTACHARYA

to the
DEPARTMENT OF ELECTRICAL ENGINEERING
INDIAN INSTITUTE OF TECHNOLOGY KANPUR
AUGUST, 1983

17189

Dedicated to
SRI SRI RAMKRISHNA PARAMHANSA DEV

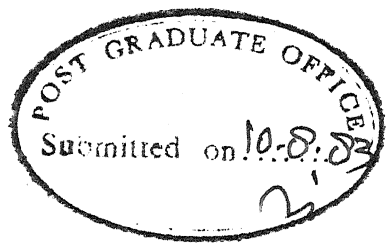
26 MAY 1984

CENTRAL LIBRARY

Accession No.

82481

EE-1983-M-BHA-DIG



CERTIFICATE

It is to certify that this work entitled
'DIGITAL SIMULATION OF TWELVE PULSE CONVERTER' by
Suborto Bhattacharya has been carried out under my
supervision and that this work has not been submitted
elsewhere for the award for a degree.

A handwritten signature in cursive script, appearing to read "K.R. Padiyar".

Dr. K.R. Padiyar
Professor
Department of Electrical Engineering
Indian Institute of Technology
Kanpur, India.

ACKNOWLEDGEMENTS

I wish to put on record my deepest sense of regard to my parents and grand-parents who inspired me to undertake this venture.

Although the responsibility for the present thesis rests on me, yet, the name of my teacher and supervisor Prof. K.R. Padiyar needs a special mention whose decisive influence on this work is foremost. Any attempt on my part to express my acknowledgement would be fatuous - and impossible. To him, I owe a debt of especial gratitude. My heartfelt thanks to Prof. L.P. Singh for the constant encouragement throughout my stay at IIT, Kanpur.

I am indebted to Shri Sachchidanand for the help and advice he rendered throughout my work. I thank my friends S/Shri V.P. Sunnak, Biswajit, Poolak, Gouri, H.K. Patel, A. Anwar, R.L. Verma, H.S.Y. Shastri and Desikachar for many fruitful discussions and the co-operation they have rendered during my M.Tech. programme.

Special thanks goes to Shri A.G. Kothari for helping me to debug the computer program and to Uma for her not so infrequent fights with me.

Financial assistance received from the Department of Science and Technology, Govt. of India is gratefully acknowledged.

Thanks are due to M/s. Triveni Tiwari and Gangaram for fast and careful cyclostyling.

To my friend Senthil, who always helped me at the cost of his own work, to whom I offer nothing but an inadequate acknowledgement of my appreciation and finally to my sisters Mithu and Putul for obvious reasons.

SUBROTO BHATTACHARYA
Aug. 9, 1983

CONTENTS

	Page
CHAPTER 1	
INTRODUCTION	1
1.1 General	1
1.2 Review	2
1.3 The objective of the thesis	5
1.4 Outline of thesis	6
CHAPTER 2	
MATHEMATICAL MODELLING OF A 12-PULSE CONVERTER	8
2.1 Introduction	8
2.2 Converter representation	8
2.2.1 Extension of the model to 12-pulse converter	19
2.3 Converter control	23
2.3.1 Firing control scheme with IPC	23
2.3.2 Firing control scheme with EPC	25
2.4 Representation of DC network	27
2.5 Conclusion	27
CHAPTER 3	
SIMULATION OF HVDC LINK	28
3.1 Introduction	28
3.2 Computer program	28
3.3 Test simulation	31
3.3.1 Steady state response	31
3.3.2 Transient response	33
3.4 Conclusion	38

	Page
CHAPTER 4 SIMULATION OF HVDC LINK WITH AC REPRESENTATION	44
4.1 Introduction	44
4.2 AC system model	44
4.3 Interfacing the converter and ac system	46
4.4 Test simulation	49
4.4.1 Steady state response	49
4.4.2 Effect of harmonic filters	51
4.4.3 Transient response	60
4.5 Conclusion	63
CHAPTER 5 CONCLUSION	69
REFERENCES	72
APPENDIX A	A1
APPENDIX B	B1
APPENDIX C	C1

LIST OF FIGURES

Fig.No.	Caption	Page
2.1	Three phase bridge converter system	10
2.2	Directed graph of a 6 pulse bridge	11
2.3	Model of a 6 pulse bridge	11
2.4	Equivalent circuit of 6 pulse converter	17
2.5	Transformer connection for 12 pulse operation	17
2.6	Interconnection of two equivalent circuit model of 6 pulse converter to form equivalent circuit model of 12 pulse converter	21
2.7	Reduced equivalent circuit model of 12 pulse converter	21
2.8	Equidistant pulse control	26
3.1	Flow-chart of the program	29
3.2	Two terminal HVDC system	32
3.3	Steady state waveforms for 6 pulse converter	34
3.4	Steady state waveforms of 12 pulse converter	35
3.5	Commutation failure due to voltage dip at the inverter terminal	36
3.6	Shows the commutation failure in the bridges (12 pulse converter)	37
3.7	Case A(i)	39
3.8	Case B(i)	40
3.9	Case A(ii)	41
3.10	Case B(ii)	42

Fig.No.	Caption	Page
4.1	AC system representation	45
4.2	Interface between AC system and converter model	48
4.3	Single terminal HVDC system feeding a constant voltage source	50
4.4	Steady state waveforms for single terminal system with ac system (SCR = 15) and filters, IPC firing scheme	52
4.5	Steady state waveforms for single terminal system with ac system (SCR = 15) and filters, EPC firing scheme	53
4.6	Steady state waveforms for single terminal system with ac system (SCR = 15) and without filters, IPC firing scheme	54
4.7	Steady state waveforms for single terminal system with AC system (SCR = 15) and without filters, EPC firing scheme	55
4.8	AC voltage and current waveforms (IPC and filter)	56
4.9	AC voltage and current waveforms (IPC without filter)	57
4.10	AC voltage and current waveforms (EPC : and filter)	59
4.11	AC voltage and current waveforms (EPC without filter)	59
4.12	Variation of DC voltage and current with filter and IPC firing scheme (SCR = 15)	61
4.13	Variation in dc voltage and current with filter and IPC firing scheme (SCR = 15)	62

Fig.No.	Caption	Page
4.14	Case A(i)	64
4.15	Case A(ii)	65
4.16	Case B(i)	66
4.17	Case B(ii)	67
B.1	Series tune filter	B3
B.2	Second-order high pass filter	B3

ABSTRACT

In this thesis a model of a 12 pulse converter is described for dynamic digital simulation of HVDC system. Both constant current and constant extinction angle controls are represented in detail.

A computer program has been developed based on these models, for the digital simulation of a two terminal HVDC system with six or twelve pulse converters at both ends. In addition to the converter and its controls DC and AC system along with filters are also represented in detail.

Test simulations are carried out both for steady state and transient conditions to illustrate controller performance.

CHAPTER 1

INTRODUCTION

1.1 GENERAL

Despite the general acceptance of ac transmission, dc transmission made its successful beginning in 1954 with the Gotland link (Sweden), leading to an awakening of interest in HVDC transmission. The advent of thyristors and other solid state devices made converter control simple and reliable thus, significantly adding to the advantages of dc transmission. Hence, in recent years, HVDC transmission has become a viable alternative over ac transmission for i) bulk power long distance transmission and ii) inter-connection of ac systems.

To augment the existing power system with dc link, the study of operation and control of HVDC systems for planning and design of composite ac/dc system becomes necessary. These studies are usually conducted on HVDC simulator. However, the HVDC simulator has less flexibility and involves increased cost in representing wider range of system configuration and control schemes. This has given rise to the development of analytical techniques and digital simulation. The extent of mathematical modelling of HVDC system depends on the nature

of study. Before describing the objectives and outline of this thesis a brief review of the literature pertaining to digital simulation of HVDC systems is presented.

1.2 REVIEW

Dynamic digital simulation involves the study of system responses over a wide range of frequency ranging from fundamental to higher, both under normal and abnormal conditions. Since the converter has a time varying topology (i.e. the conduction pattern changing with the firing of the valve and its cessation), the major difficulty lies in representing the converter to suit the nature of studies.

There are two approaches to the problem of handling the time varying topology of the converter.

The first method is based on the use of tensor analysis technique [1]. Based on the conduction pattern, a transformation matrix is generated by the digital computer, using which converter dynamic equations corresponding to each state of the converter are formulated. Hingorani et al. [2] represented a two terminal dc link based on this approach. Later, Hay et al. [3] introduced a general method for representing a multiconverter system for two terminal dc link. Williams et al. [4] have formed the loop impedance matrix of the converter network assuming all the valves of the bridge to be conducting. Depending on the conduction pattern of the converter the loop impedance matrix is

reduced to get the connection matrix. Vovus et al. [5] extended the above method to simulate 12 pulse 2 terminal HVDC system. Padiyar et al. [6] represented the converter based on graph theoretic approach, assuming the dc link current to be continuous. The topological analysis leads directly to the derivation of converter dynamic equations and expressions for dependent variables such as valve voltages.

The second method is based on the storing the sets of differential equations describing the converter topology for different valve conduction patterns. Corresponding to the conduction state, the appropriate set of equations is chosen at any given time. El-Serafi et al. [7] formulated a set of five general equations in phase quantities for the normal modes of operation of a converter. The equation for the particular mode of operation is obtained by substituting certain empirical conditions in the general equations. In the central process method of Hingorani et al. [8], a central process starts from the instant of firing a valve and continues upto the instant of next firing. The continuous converter operation is simulated by successive use of the central process which is a set of differential and boolean equations. Depending upon the state of converter the appropriate differential equations are selected and solved. The method has been used to simulate a two terminal dc link

assuming normal converter operation. Htsui et al. [9] modelled a converter by formulating a set of generalised differential equations which are derived corresponding to all the possible normal combinations of conducting valves.

There is an alternative approach whereby the converter is represented by a network of fixed topology but time varying impedances [10].

A valve is represented by high impedance when it is off and low impedance when it is on. Though this method is conceptually simple, it needs a small integration step size for the solution of the converter state equations due to time dependent impedances.

The design of control system is one of the aims of dynamic digital simulation. Very few papers have dealt with this aspect in detail. References [2,5,8] algebraically relate firing angle to the current error. This simplification may not be adequate when ac system is represented in detail. Reeve et al. [11] modelled constant current controller and extinction angle controller based on pulse phase control firing scheme and illustrated their capability by simulating a multiterminal HVDC system under transient conditions. Padiyar et al. [6] represented the constant current controller using individual phase control (IPC) or EPC (using pulse frequency control) firing schemes and the constant extinction

ABSTRACT

In this thesis a model of a 12 pulse converter is described for dynamic digital simulation of HVDC system. Both constant current and constant extinction angle controls are represented in detail.

A computer program has been developed based on these models, for the digital simulation of a two terminal HVDC system with six or twelve pulse converters at both ends. In addition to the converter and its controls DC and AC system along with filters are also represented in detail.

Test simulations are carried out both for steady state and transient conditions to illustrate controller performance.

CHAPTER 1

INTRODUCTION

1.1 GENERAL

Despite the general acceptance of ac transmission, dc transmission made its successful beginning in 1954 with the Gotland link (Sweden), leading to an awakening of interest in HVDC transmission. The advent of thyristors and other solid state devices made converter control simple and reliable thus, significantly adding to the advantages of dc transmission. Hence, in recent years, HVDC transmission has become a viable alternative over ac transmission for i) bulk power long distance transmission and ii) inter-connection of ac systems.

To augment the existing power system with dc link, the study of operation and control of HVDC systems for planning and design of composite ac/dc system becomes necessary. These studies are usually conducted on HVDC simulator. However, the HVDC simulator has less flexibility and involves increased cost in representing wider range of system configuration and control schemes. This has given rise to the development of analytical techniques and digital simulation. The extent of mathematical modelling of HVDC system depends on the nature

of study. Before describing the objectives and outline of this thesis a brief review of the literature pertaining to digital simulation of HVDC systems is presented.

1.2 REVIEW

Dynamic digital simulation involves the study of system responses over a wide range of frequency ranging from fundamental to higher, both under normal and abnormal conditions. Since the converter has a time varying topology (i.e. the conduction pattern changing with the firing of the valve and its cessation), the major difficulty lies in representing the converter to suit the nature of studies.

There are two approaches to the problem of handling the time varying topology of the converter.

The first method is based on the use of tensor analysis technique [1]. Based on the conduction pattern, a transformation matrix is generated by the digital computer, using which converter dynamic equations corresponding to each state of the converter are formulated. Hingorani et al. [2] represented a two terminal dc link based on this approach. Later, Hay et al. [3] introduced a general method for representing a multiconverter system for two terminal dc link. Williams et al. [4] have formed the loop impedance matrix of the converter network assuming all the valves of the bridge to be conducting. Depending on the conduction pattern of the converter the loop impedance matrix is

reduced to get the connection matrix. Vovus et al. [5] extended the above method to simulate 12 pulse 2 terminal HVDC system. Padiyar et al. [6] represented the converter based on graph theoretic approach, assuming the dc link current to be continuous. The topological analysis leads directly to the derivation of converter dynamic equations and expressions for dependent variables such as valve voltages.

The second method is based on the storing the sets of differential equations describing the converter topology for different valve conduction patterns. Corresponding to the conduction state, the appropriate set of equations is chosen at any given time. El-Serafi et al. [7] formulated a set of five general equations in phase quantities for the normal modes of operation of a converter. The equation for the particular mode of operation is obtained by substituting certain empirical conditions in the general equations. In the central process method of Hingorani et al. [8], a central process starts from the instant of firing a valve and continues upto the instant of next firing. The continuous converter operation is simulated by successive use of the central process which is a set of differential and boolean equations. Depending upon the state of converter the appropriate differential equations are selected and solved. The method has been used to simulate a two terminal dc link

assuming normal converter operation. Htsui et al. [9] modelled a converter by formulating a set of generalised differential equations which are derived corresponding to all the possible normal combinations of conducting valves.

There is an alternative approach whereby the converter is represented by a network of fixed topology but time varying impedances [10].

A valve is represented by high impedance when it is off and low impedance when it is on. Though this method is conceptually simple, it needs a small integration step size for the solution of the converter state equations due to time dependent impedances.

The design of control system is one of the aims of dynamic digital simulation. Very few papers have dealt with this aspect in detail. References [2,5,8] algebraically relate firing angle to the current error. This simplification may not be adequate when ac system is represented in detail. Reeve et al. [11] modelled constant current controller and extinction angle controller based on pulse phase control firing scheme and illustrated their capability by simulating a multiterminal HVDC system under transient conditions. Padiyar et al. [6] represented the constant current controller using individual phase control (IPC) or EPC (using pulse frequency control) firing schemes and the constant extinction

angle controller using IPC scheme. They validated the models by performing transient studies on a multiterminal HVDC system.

Vovas et al. [5] considered the detailed representation of ac system and simulated ac line faults on a parallel ac/dc link connecting two areas. Each area includes detail representation of synchronous machine. El-Serafi [7] investigated the transient behaviour of a synchronous machine connected to a converter. Hay et al. [3] represented the ac system as a simple impedance calculated from the short circuit ratio (SCR) at the converter bus and the impedance angle of the ac system. In the references [2,5,7] the harmonic filters have also been included in simulation. The study of harmonic interaction between the ac and dc systems is reported in the papers [12,13].

1.3 THE OBJECTIVE OF THE THESIS

The objectives of the thesis are

- i) to report a methodology of representing a HVDC converter based on equivalent circuit approach using graph theoretic analysis. This representation can be used for 6 as well as 12 pulse converter;

- ii) to develop a digital computer program to simulate a two terminal dc link based on the proposed converter model and with detailed representation of such as converter controls, DC and AC system alongwith filters;
- iii) to simulate a two terminal HVDC system under both steady state and transient conditions and to observe the effect of IPC and EPC firing schemes on the system response using the computer program.

1.4 OUTLINE OF THE THESIS

The chapterwise summary of the thesis is as follows :

- i) Chapter 2 deals with model formulation of dc sub-system consisting of the converter, dc line, current controller and the extinction angle controller.
- ii) Description of the development of the computer program alongwith its flow-chart is given in the Chapter 3. Steady state and transient performance of a HVDC link without detailed ac system representation have been presented.
- iii) The state space model of the ac system and harmonic filters is developed in Chapter 4. The converter is treated as a dependent current source for the ac system whose effect is represented as a dependent voltage source in the converter model. In interfacing the ac and dc side variables the identity of transformer connection and tap is maintained. The computer program

developed in the Chapter 3 is augmented to include the ac system model and its capability is validated using single and two terminal HVDC system. The effect of harmonic filters and effectiveness of IPC and EPC firing schemes on the system performance are studied.

- iv) Chapter 5 . reviews the major contribution of the thesis and gives the future scope of work.

CHAPTER 2

MATHEMATICAL MODELLING OF A 12-PULSE CONVERTER

2.1 INTRODUCTION

A HVDC system mainly consists of (i) the ac system feeding the converter (ii) converters with their associated controls and (iii) the DC network consisting of transmission lines. Each component is modelled separately and in a modular fashion. The individual component models are interfaced using appropriate variables.

This chapter deals with the 12-pulse converter representation alongwith its associated control system. The converter is modelled as a variable voltage source behind a variable impedance. The formulation of the converter equations corresponding to all the possible modes, with the assumption of continuous dc link current, becomes simple using graph theoretic approach. The converter equations are formulated using cut set matrix and the constituent equations for the elements of the associated graph. The dynamics of the converter control using both individual phase control and equidistant pulse control firing schemes, are represented and simulated in detail.

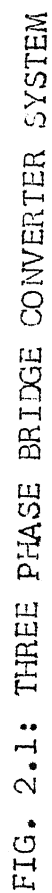
2.2 CONVERTER REPRESENTATION

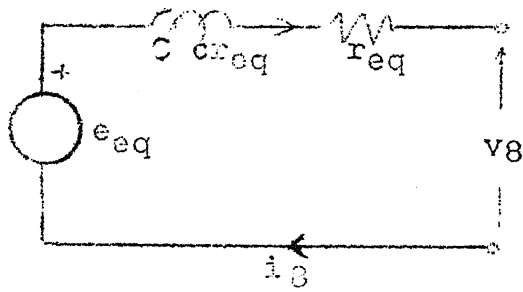
The modelling of the 12-pulse converter has been

achieved through the modelling of the individual 6-pulse converter unit. Since, the extension of the 6-pulse converter model is dealt later in this article, the formulation of 6-pulse converter model is taken up first.

A three phase bridge converter system is shown in Fig. 2.1. This includes the resistances and inductances of the converter transformer (R_a, R_b, R_c and L_a, L_b, L_c) and the dc smoothing reactor (R_d, L_d). Both the ac and the dc voltage sources are not constant and are actually the output of ac and dc network models. The effect of the converter on the ac and dc networks are represented by the injection of currents into the respective network.

The graph associated with the converter of Fig. 2.1 is shown in Fig. 2.2. In total there are 9 elements of which, the first 6 represents the values and the orientation of each of these is along that of the direction of current flow in the valve. Elements 7 and 9 correspond to the equivalent circuit representation [1] of the ac system feeding the converter. The element 8 includes the series combination of R_d, L_d and V_c . In deriving the graph of Fig. 2.2 the grading and damping circuits across the valves are ignored. The tree of the graph in Fig. 2.2 will have 4 elements. Although there is no unique tree for a graph, in what follows elements 7 and 9 are chosen as two of the elements of the tree. In addition, any two of the conducting





11

Fig. 2.3 Model of a 6 pulse bridge

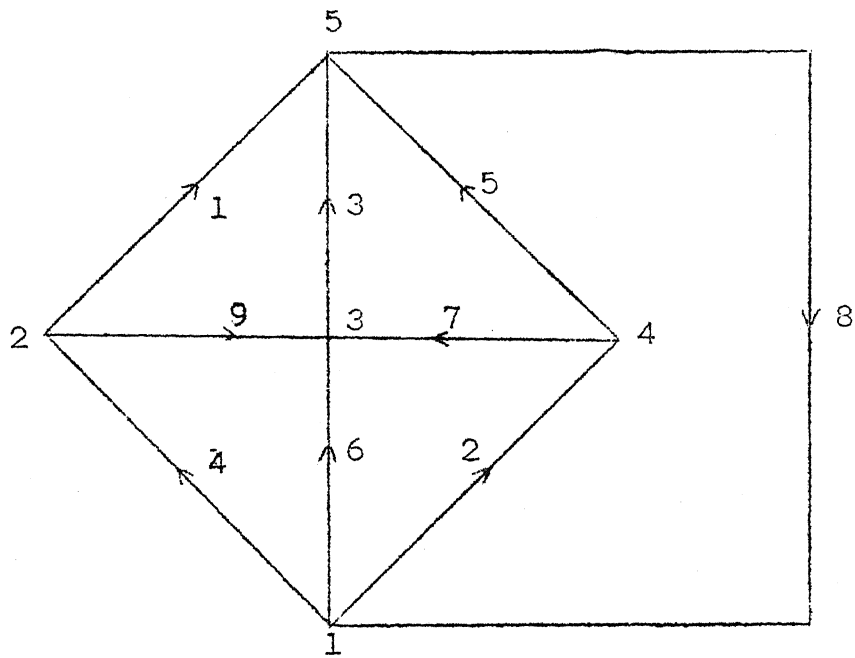


FIG. 2.2: DIRECTED GRAPH OF A 6 PULSE BRIDGE

valve elements are included in the tree. (It is to be noted that there are, always, at least two valves conducting i dc current is to be continuous.

The constituent equations of elements 7 and 9 can be written as

$$\underline{v}_{T1} = \underline{Z}_{11} \underline{i}_{T1} + \underline{e}_{11} \quad (2.1)$$

and that of element 8 is

$$v_8 = Z_8 i_8 + e_8 \quad (2.2)$$

where

$$\underline{v}_{T1} = [v_7 \ v_9]^T, \quad v_j \text{ is the voltage across the element } j$$

$$\underline{i}_{T1} = [i_7 \ i_9]^T, \quad i_j \text{ is the current through element } j$$

$$Z_8 = R_d + L_d p$$

$$e_8 = V_c$$

and

$$\underline{e}_{11} = [e_c - e_b \ e_a - e_b]^T$$

the superscript T indicates transpose and e_a, e_b and e_c are line to neutral ac voltages of phases a, b and c respectively,

$$Z_{11} = R_{11}(1+cp)$$

Here c, p and R_{11} are defined as

$$c = \frac{L_a}{R_a} = \frac{L_b}{R_b} = \frac{L_c}{R_c}, \quad p \equiv d/dt$$

$$R_{11} = \begin{bmatrix} R_a + R_b & R_b \\ R_b & R_c + R_b \end{bmatrix}$$

c , the time constant of source impedance is assumed to be the same in all the phases.

The elements 1 to 6 represent the valves and are governed by the following equations;

$$v_k = 0 \quad \text{if the valve is conducting} \quad (2.3)$$

$$i_k = 0 \quad \text{if the valve is non-conducting}$$

v_k and i_k are the voltage across and the current through the valve.

From graph theory, the branch and link variables are related by the following expressions

$$\begin{bmatrix} i_{T1} \\ i_{T2} \end{bmatrix} = -B \begin{bmatrix} i_8 \\ i_{L2} \\ i_{L3} \end{bmatrix} \quad (2.4)$$

$$\begin{bmatrix} v_8 \\ v_{L2} \\ v_{L3} \end{bmatrix} = B^T \begin{bmatrix} v_{T1} \\ v_{T2} \end{bmatrix} \quad (2.5)$$

where subscript T and L refer to branches and links respectively. B is the fundamental cutset matrix corresponding to link elements.

The tree branches are partitioned into two sets, one set (T_1) consisting of elements 7 and 9 and the other (T_2) consisting of the conducting valves. The link elements are partitioned into 3 sets. The first set (L_1) corresponds to element 8 and the other two sets (L_2 and L_3) consist of conducting and non-conducting valves in the links respectively. The matrix B can then be partitioned as

$$B = \begin{array}{c} \begin{array}{cc} & \begin{array}{ccc} L_1 & L_2 & L_3 \end{array} \\ \begin{array}{c} T_1 \\ T_2 \end{array} & \begin{bmatrix} B_{L11} & B_{L12} & B_{L13} \\ B_{L21} & B_{L22} & B_{L23} \end{bmatrix} \end{array}$$

Using (2.3) in conjunction with (2.4) and (2.5) it follows that

$$\begin{aligned} i_{L3} &= 0 \\ v_{T2} &= 0 \\ v_{L2} &= 0 \end{aligned} \quad (2.6)$$

Expanding equations (2.4) and (2.5) and using (2.6), the following relations are obtained

$$i_{T1} = -B_{L11}i_8 - B_{L12}i_{L2} \quad (2.7)$$

$$i_{T2} = -B_{L21}i_8 - B_{L22}i_{L2} \quad (2.8)$$

$$v_8 = B_{L11}^T v_{T1} \quad (2.9)$$

$$v_{L2} = 0 = B_{L12}^T v_{T1} \quad (2.10)$$

$$v_{L3} = B_{L13}^T v_{T1} \quad (2.11)$$

Equation (2.9) can be modified using (2.7) and (2.1) as

$$v_8 = -Z_1 i_8 - Z_2 i_{L2} + B_{L11}^T e_{11} \quad (2.12)$$

and i_{L2} can be written by using (2.10), (2.7) and (2.1) as

$$(1+cp)i_{L2} = -R_4^{-1}Z_3 i_8 + R_4^{-1}B_{L12}^T e_{11} \quad (2.13)$$

where

$$Z_1 \triangleq B_{L11}^T R_{11} B_{L11} (1+cp) = R_1 (1+cp)$$

$$Z_2 \triangleq B_{L11}^T R_{11} B_{L12} (1+cp) = R_2 (1+cp)$$

$$Z_3 \triangleq B_{L12}^T R_{11} B_{L11} (1+cp) = R_3 (1+cp)$$

$$Z_4 \triangleq B_{L12}^T R_{11} B_{L12} (1+cp) = R_4 (1+cp)$$

Equation (2.12) can be further simplified by using (2.13) to get

$$v_8 = -Z_{eq} i_8 + e_{eq} \quad (2.14)$$

where

$$Z_{eq} \triangleq (R_1 - R_2 R_4^{-1} R_3)(1+cp) = r_{eq}(1+cp)$$

$$e_{eq} \triangleq (B_{L11}^T - R_2 R_4^{-1} B_{L12}^T) e_{11}$$

v_8 is the voltage across the element 8, which is the dc voltage before the smoothing reactor of the bridge. Thus, using (2.14) an equivalent circuit (Fig. 2.3) can be formed where Z_{eq} and e_{eq} are the impedance and voltage source respectively in the equivalent circuit.

The complete model of a 6-pulse converter is thus as shown in Fig. 2.4. The dynamic equation which gives the dc current of the converter is

$$\frac{di_8}{dt} = -\frac{R}{L} i_8 + (e_{eq} - V_c)/L \quad (2.15)$$

where

$$R = r_{eq} + R_d ; L = c r_{eq} + L_d$$

In addition to (2.15), equation (2.13) has to be solved for the case of three and four valve conduction mode. The currents in the conducting valves in the branches and links are given by the equations (2.8) and (2.13) respectively, whereas the voltage across the non-conducting valves is given by the equation (2.11).

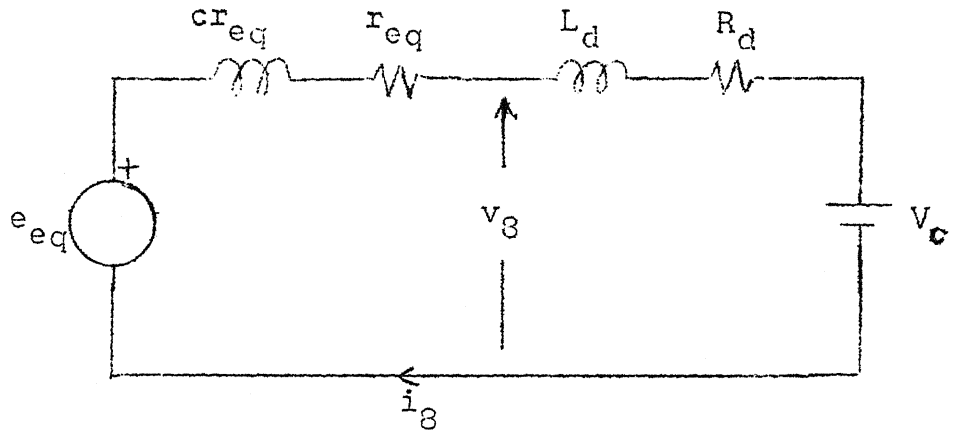


FIG. 2.4: EQUIVALENT CIRCUIT OF 6 PULSE CONVERTER

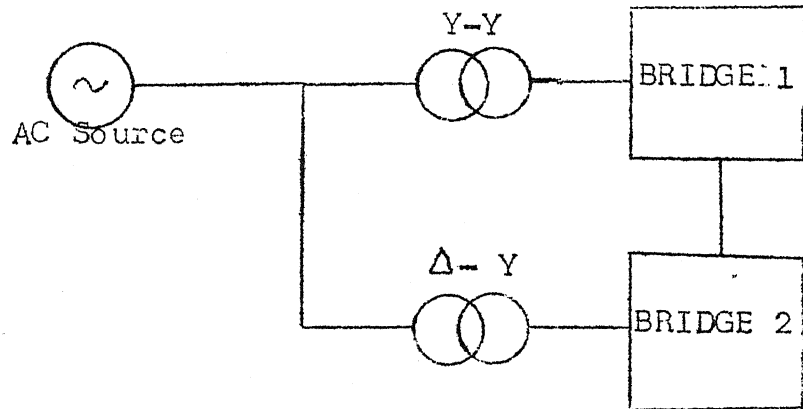


FIG. 2.5: TRANSFORMER CONNECTION FOR 12 PULSE OPERATION

Example :

An example of 3 valve conduction mode is taken up to illustrate the above analysis. Assuming that the valves 1, 2 and 3 are conducting and out of which the valves 2 and 3 are in the branches (set T_2) and the valve 1 in the link. The remaining valves form the non-conducting set, L_3 . The matrix B is partitioned accordingly and is shown below.

$$P = B = \begin{array}{c} \begin{array}{cc} & \begin{array}{ccccc} 8 & 1 & 6 & 5 & 4 \end{array} \\ \begin{array}{c} T_1 \\ T_2 \\ L_3 \end{array} & \begin{array}{ccc|ccc} 7 & -1 & 0 & 1 & 1 & 1 \\ 9 & 0 & 1 & 0 & 0 & -1 \\ \hline 2 & -1 & 0 & 1 & 0 & 1 \\ 3 & -1 & 1 & 0 & 1 & 0 \\ \hline & L_1 & L_2 & & L_3 & \end{array} \end{array}$$

R_1, R_2, R_3 and R_4 can be computed from the expressions defined above. Thus, the equivalent circuit parameters are

$$r_{eq} = R_1 - R_2 R_4^{-1} R_3 = R_a + R_b - R_b^2 / (R_b + R_c)$$

$$e_{eq} = e_c - e_b + R_x (e_a - e_b), \text{ where } R_x = R_b / (R_c + R_b)$$

From the knowledge of the sub-matrices of the matrix B and knowing r_{eq} and e_{eq} , the dynamic equation giving the current through the conducting valves in the link is

$$pi_{L2} = -i_{L2}/c + R_x(i_c/c + pi_3) + (e_a - e_b)/c(R_b - R_c)$$

and the dynamic equation for the dc current of the converter

$$pi_3 = -\frac{R}{L} i_3 + (e_{eq} - V_c)/L$$

R and L are defined earlier.

The expressions of the currents through the conducting valves in the tree and the voltages across the non-conducting valves are

$$i_2 = i_3$$

$$i_3 = i_3 - i_{L2}$$

$$V_6 = V_5 = (R_a + R_b)(i_3 + cpi_3) - R_b(i_{L2} + cpi_{L2}) + e_c - e_b$$

$$V_4 = R_a(i_3 + cpi_3) + R_c(i_{L2} + cpi_{L2}) + e_c - e_a$$

These are computed after solving the dynamic equations.

2.2.1 Extension of the model to 12-pulse converter

Two six pulse bridge in series constitutes a 12-pulse converter. Power to each of the bridges are supplied from two transformers, one having wye/wye connection and the other

delta/bye as shown in Fig. 2.5. The above mode of transformer connection is adopted in order to produce two sets of voltages having a relative phase difference of 30 degrees between the corresponding phases. Each 6 pulse bridge can be represented by the equivalent circuit of Fig. 2.3 and the series connection of two such circuits with L_d, R_d and V_c gives the model for 12 pulse converter shown in Fig. 2.6. The circuit in Fig. 2.6 can be reduced to that of Fig. 2.7. The equivalent circuit parameters of this reduced 12 pulse converter model are given by

$$E_{eq} = \sum_{j=1}^2 e_{eqj}$$

$$R_{eq} = \sum_{j=1}^2 r_{eqj}$$

$$L_{eq} = \sum_{j=1}^2 c_j r_{eqj}$$

where e_{eqj} and r_{eqj} are equivalent circuit parameters for the bridge j .

The primary dynamic equation of the 12 pulse converter is

$$\frac{di_8}{dt} = -\frac{R'}{L'} i_8 + (E_{eq} - V_c)/L' \quad (2.16)$$

where $L' = L_{eq} + L_d$; $R' = R_{eq} + R_d$.

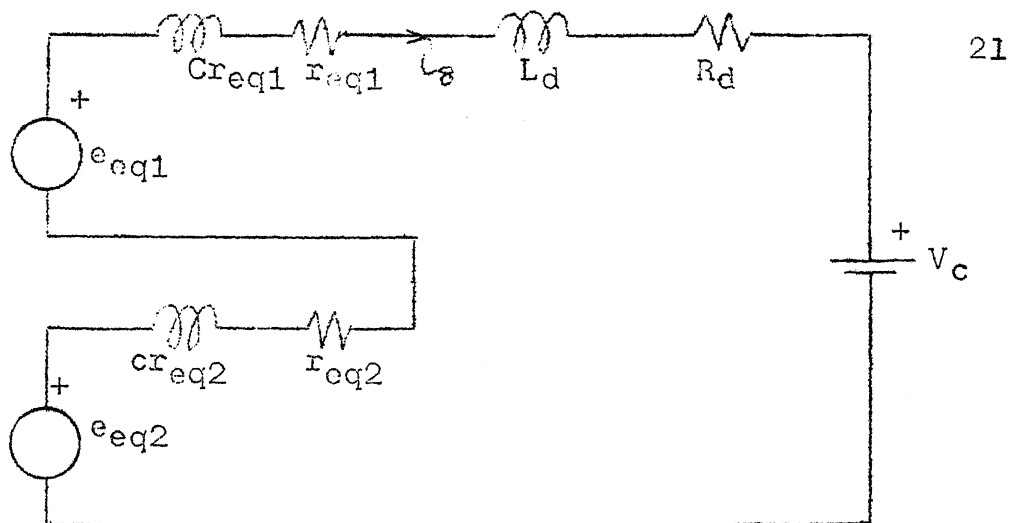


Fig. 2.6 INTERCONNECTION OF TWO EQUIVALENT CIRCUIT MODELS OF 6 PULSE CONVERTER TO FORM 12 PULSE CONVERTER

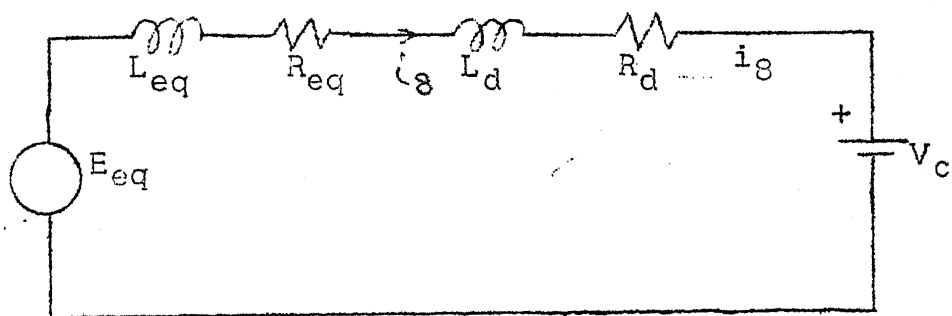


Fig. 2.7 REDUCED EQUIVALENT CIRCUIT MODEL OF 12 PULSE CONVERTER

The equation (2.16) is of the same form as (2.15) except for the change in the equivalent circuit parameters. At every instant, (2.16) has to be solved for the 12-pulse converter and for each 6 pulse bridge, (2.13) has to be solved. The matrix B associated with each bridge changes whenever a valve ceases or commences conduction. The new matrix B is computed each time depending on the tree elements.

The procedure outlined above can be compared with the method described in [2,4,6] which are similar in objective. The method given here is simpler both conceptually and computationally. The main difference of this 6 pulse model with [6] is that the present model can be easily extended to represent a 12 pulse converter. Inclusion of a different valve characteristic such as finite impedance during the non-conducting period of the valves other than that of an ideal switch can also be accomplished. In doing so, the constituent equation (2.1) would be different. In contrast, the reference [2,4] implicitly assume that the valve impedance is infinite when it is non-conducting. The number of state equations per converter terminal will vary depending on the number of conducting valves per bridge (N_i) and is given by $1 + \sum_{i=1}^b (N_i - 2)$, where b is the number of bridges per converter terminal.

2.3 CONVERTER CONTROL

Each converter in a HVDC system is equipped with a controller that determines the instant of firing of each valve. The firing pulses are generated from a control signal which is the output of the current or extinction angle controllers. Normally current control is used at the rectifier and constant extinction angle (CEA) at the inverter. Basically, there are two firing control schemes :

- i) Individual phase control (IPC), where the firing pulse for each valve is determined with respect to its own commutation voltage.
- ii) Equidistant pulse control (EPC), where the controller generates pulses at equal intervals independent of the distortion in the ac voltage waveforms.

2.3.1 Firing Control Scheme with IPC

The details of this firing pulse generation scheme are described in reference [15] for analogue implementation. The same concept, for pulse generation is used here on the digital computer. A converter is generally equipped with both constant extinction angle controller and constant current controller in order to permit change in the mode of operation.

The control signal of the converter as derived in reference [15] is

$$E_c = \int_{-\pi+\gamma_c}^{wt} e_{cj}(\tau) d\tau + 2X_c I_d + V_{cc} \quad (2.17)$$

where e_{cj} is the commutation voltage for valve j , X_c is the commutating reactance and I_d is the dc current. V_{cc} is the output of the first order current controller, expressed as

$$V_{cc} = \frac{K}{1+T_c p} (I_{ref} - I_d) \quad (2.18)$$

where K is the controller gain, T_c is the controller time-constant and I_{ref} is the current reference. The state equation of the controller can be written from the equation (2.18) and solved for V_{cc} .

Owing to harmonics, the ac voltage at the converter bus may not be sinusoidal. Thus, for the purpose of simulation the numerical integration is employed to evaluate the integral in equation (2.17). However, in case of sinusoidal ac voltages a closed form expression can be derived for the integral [15].

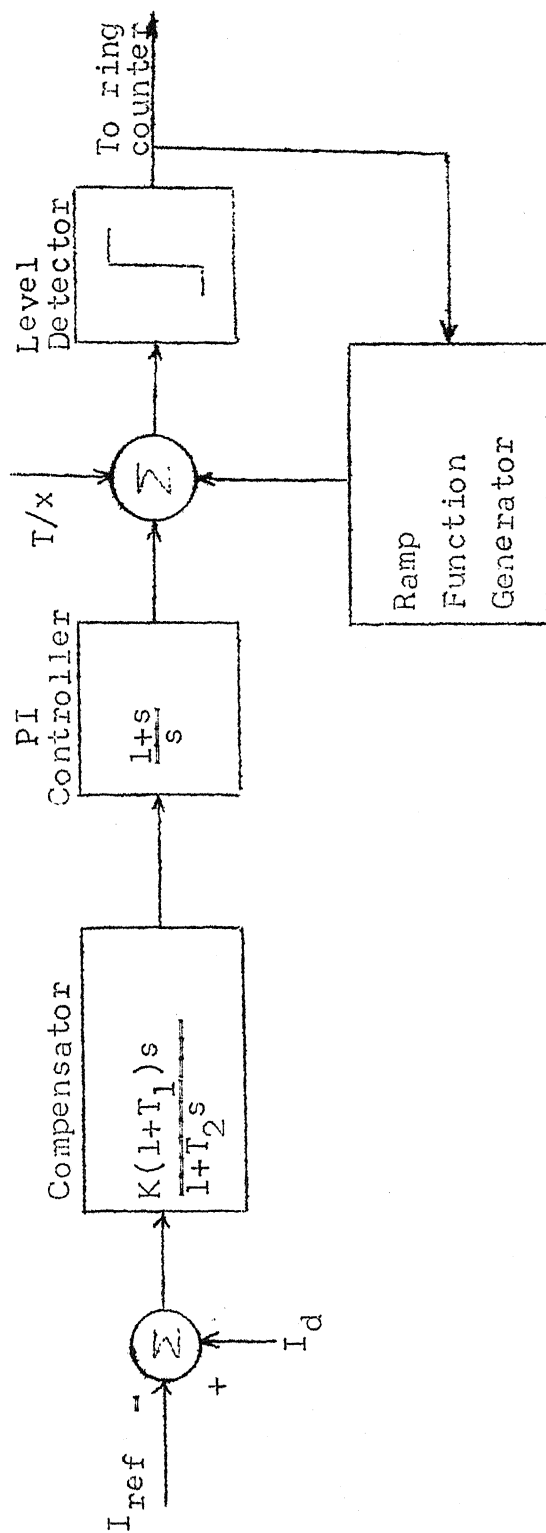
The firing pulse is initiated at the positive going zero crossing of the control signal E_c . To ensure minimum extinction angle operation of the converter, the voltage, V_{cc} is clamped to zero while going negative. With increase in V_{cc} , the angle of advance (β) increases for the converter and

if V_{cc} is large enough, β may increase to 180° . Hence, the control of the converter is over the full range of operation (rectification and inversion). In some extreme cases, there lies a possibility of the signal V_{cc} becoming larger thus forcing the control signal E_c to be positive always. This is taken care of by adding a negative pulse of duration equal to minimum delay angle (α_{min}) to the negative peak of the integral in equation (2.17). The amplitude of the pulse is large enough to ascertain that the control signal E_c goes negative for atleast the duration of the pulse and ensuring a minimum delay angle for the converter.

2.3.2 Firing Control Scheme with EPC

An equidistant pulse firing scheme with pulse frequency control has been suggested to overcome the problem of harmonic instability which is inherent with IPC [16]. In the present context of simulation, only rectifier terminal is equipped with EPC. Fig. 2.8 shows a simplified block diagram of the controller from which the state equation can be written down.

A constant slope ramp function is generated starting from zero at each firing instant. The ramp function is compared to the sum of the control signal (v_c) and the bias voltage and pulse is initiated at the instant of equality. The bias voltage is a voltage proportional to $T/6$ in case of



If 6 pulse operation $x = 6$
 If 12 pulse operation $x = 12$

FIG. 2.8: EQUIDISTANT PULSE CONTROL

6 pulse operation and $T/12$ in case of 12 pulse operation, where T is the time period of ac voltage. When $v_c = 0$, which corresponds to the steady-state operation, the firing pulses are generated at every 60° or 30° depending on 6 or 12 pulse operation respectively. To ensure the minimum delay angle operation for the rectifier the firing is inhibited until the commutation voltage has reached a defined minimum positive value. The details of this scheme are described in reference [17].

2.4 REPRESENTATION OF DC NETWORK

The dc network consists of transmission line which is represented by a π model. The dc current of each converter, which is obtained in terms of state variables, is injected into the dc network at converter terminals. State equations for the dc network can be easily written down and are time invariant. The voltage V_c in Fig. 2.1 is directly obtained as a capacitor voltage which is chosen as a state variable in the dc network equations.

2.5 CONCLUSION

In this chapter a model of a 12 pulse converter is developed for dynamic digital simulation. Both constant current control and constant extinction angle control are represented in detail.

CHAPTER 3

SIMULATION OF HVDC LINK

3.1 INTRODUCTION

Based on the models of the converter, its associated controls and dc network, described in the previous chapter, a digital-computer program has been developed to simulate 2 terminal HVDC link with 6 or 12 pulse converter at each terminal. Test simulations both under steady state and transient conditions have been carried out primarily to demonstrate the program capability. Commutation failure at the inverter terminal has also been simulated.

3.2 COMPUTER PROGRAM

Fig. 3.1 shows the flow-chart of the program which is written in FORTRAN and needs minimum data preparation. It has a modular structure which facilitates further program augmentation.

The dynamic equations of the entire system except those of the converter are time invariant. The time varying nature of these converter equations is due to the changes in the converter conduction pattern which occurs whenever a valve ceases or begins conduction. The two conditions which have to be satisfied, when a valve begins conduction are :

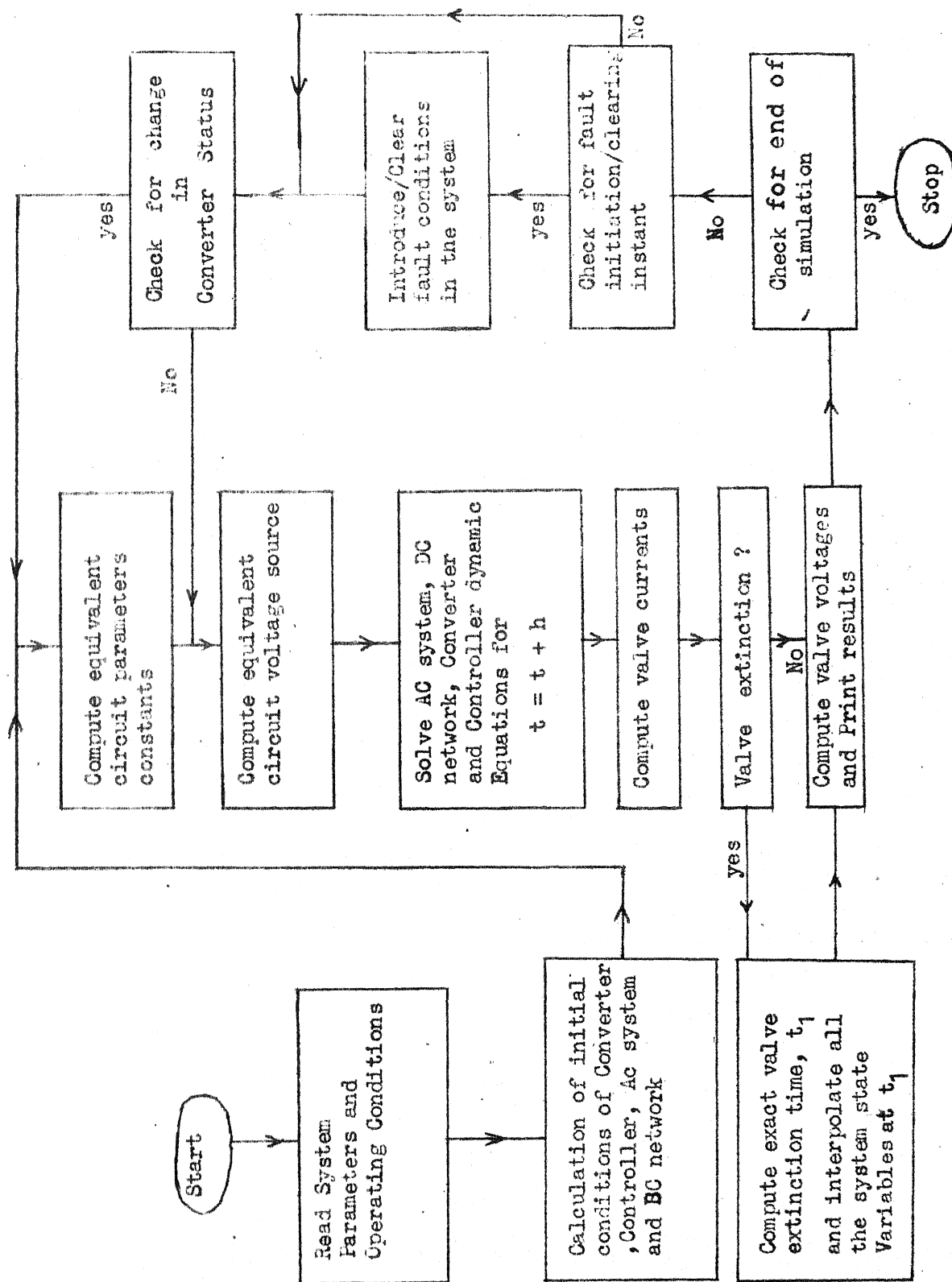


Fig. 3.1 Flow chart of the program

- i) presence of gate pulse (which is the output of the controller routine), and
- ii) positive voltage across the valve.

A valve ceases conduction if the valve current falls below zero and the exact instant of this extinction is computed by linear interpolation using valve current measurements. Each time the converter changes its status, equivalent circuit constants are evaluated (refer Chapter 2). The voltage source in the equivalent circuit is a function of the converter ac bus voltage, and hence it is computed for each time interval. Since the equivalent circuit constants are dependent on the converter conduction status, the latter is checked at the beginning of each integration time step.

The system differential equations are solved using Modified Euler method.

The salient features of the program are as follows :

- i) Both 6 pulse and 12 pulse operation of the converter can be simulated.
- ii) In its present form the program incorporate three methods of converter control which are :
 - a) constant α
 - b) constant current control
 - c) constant extinction angle control.

The firing angle control is based on either IPC or EPC scheme (see Chapter 2). However simulation, that has been carried out, the inverter operation is assumed only under IPC firing scheme (as this does not require feedback of extinction angle).

- iii) The voltage across the valve, following the cessation of its conduction is monitored for a period equal to the turn-off time. If during this period the valve gets forward biased it is put back into the conducting state.

3.3 TEST SIMULATION

A 2 terminal HVDC system, shown in Fig. 3.2, has been considered for simulation, to demonstrate the program capability. In this sample system, the rectifier (terminal 1) and the inverter (terminal 2) normally operate on constant current and constant extinction angle controls respectively. Various test simulations are conducted to investigate the system performance both under steady state and transient conditions following the disturbance. Details of the system parameters and operating conditions are given in the Appendix A.

3.3.1 Steady State Response.

The steady state waveforms for the 2 terminal system using 6 pulse converter at each terminal (operating

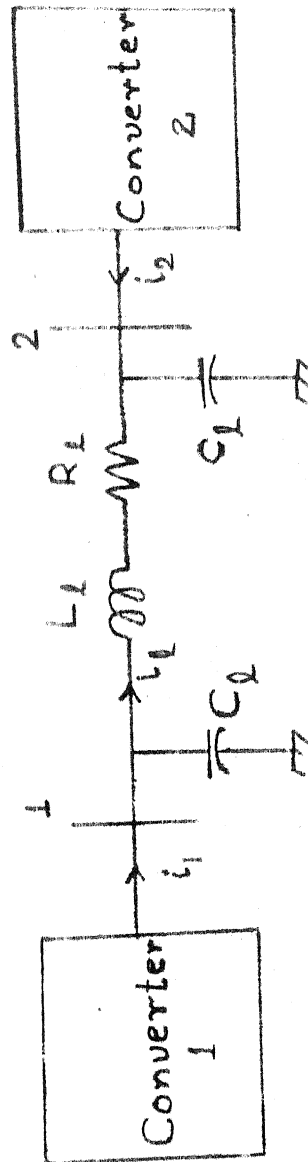


Fig. 3.2 Two Terminal HVDC system

condition A) and 12 pulse converter at each terminal (operating condition B) are shown in the Figs. 3.3 and 3.4 respectively. In either case IPC firing scheme is assumed at both the terminals. Since this study mainly illustrates the program capability, optimization of controller parameters has not been attempted. While the dc current is almost smooth for the 12 pulse converter, there is some 6th harmonic ripple for the 6 pulse converter.

3.3.2 Transient Response

Figs. 3.5 and 3.6 show the commutation failure in case of 12 pulse converter due to a 5 percent dip in ac voltage of phase B at the terminal. The dip is initiated at the start of cycle 1 and normal condition is restored at the start of cycle 2. IPC firing scheme is assumed here (operating condition B) .

The transient system responses have been studied for a 12 pulse 2 terminal system. Following disturbances were considered. Change in current reference setting (with operating condition B) using both (A) IPC and (B) EPC firing schemes.

- i) at both the terminals, from $I_{ref_1} = 1.2 \text{ p.u.}$;
 $I_{ref_2} = 1.1 \text{ p.u.}$ to $I_{ref_1} = 1.5 \text{ p.u.}$; $I_{ref_2} = 1.4 \text{ p.u.}$
- ii) at both the terminals from $I_{ref_1} = 1.2 \text{ p.u.}$;
 $I_{ref_2} = 1.1 \text{ p.u.}$ to $I_{ref_1} = 1.75 \text{ p.u.}$; $I_{ref_2} = 1.65 \text{ p.u.}$

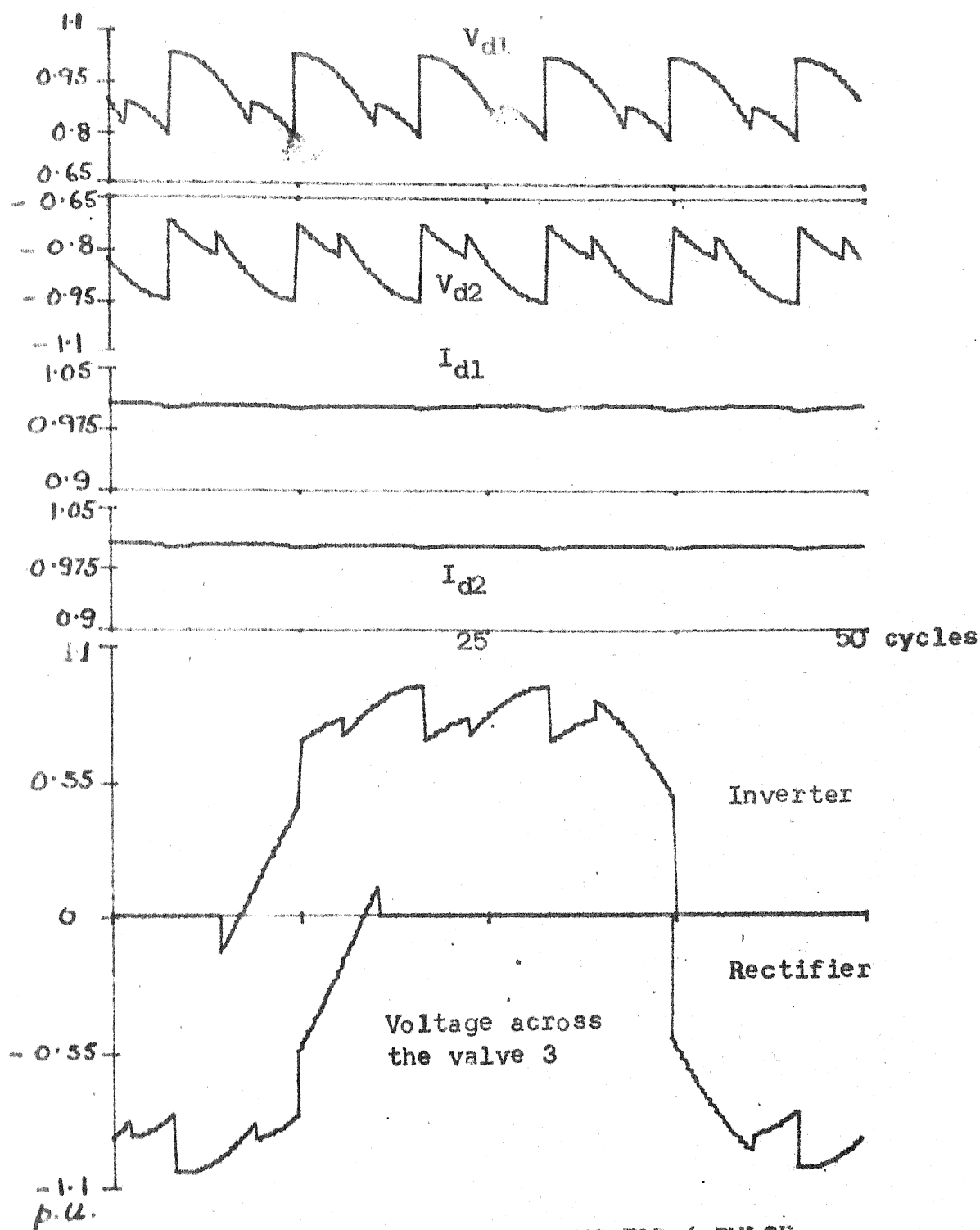


Fig. 3.3 STEADY STATE WAVEFORMS FOR 6 PULSE CONVERTER

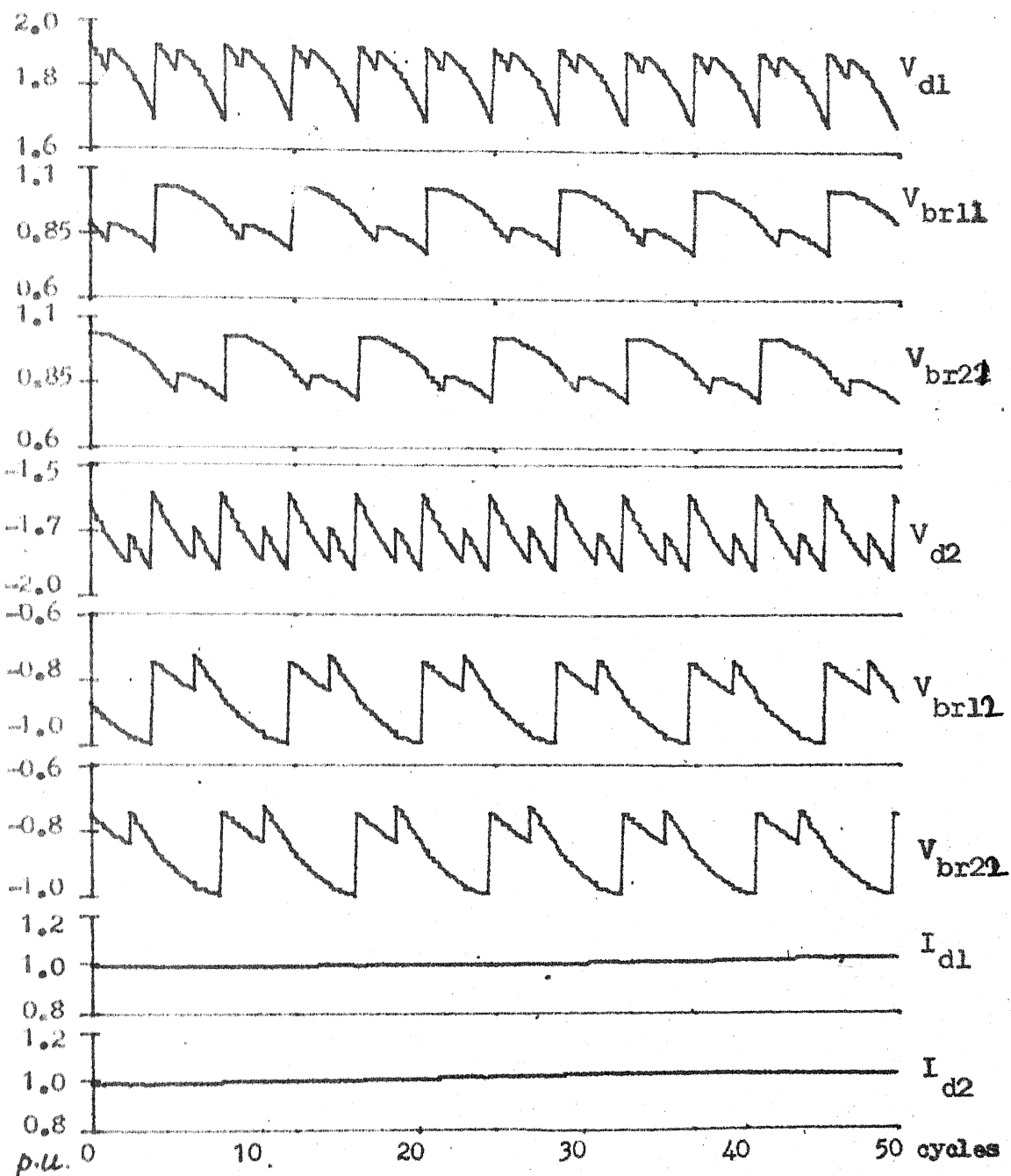


Fig. 3.4 STEADY STATE WAVEFORMS OF 12 PULSE CONVERTER

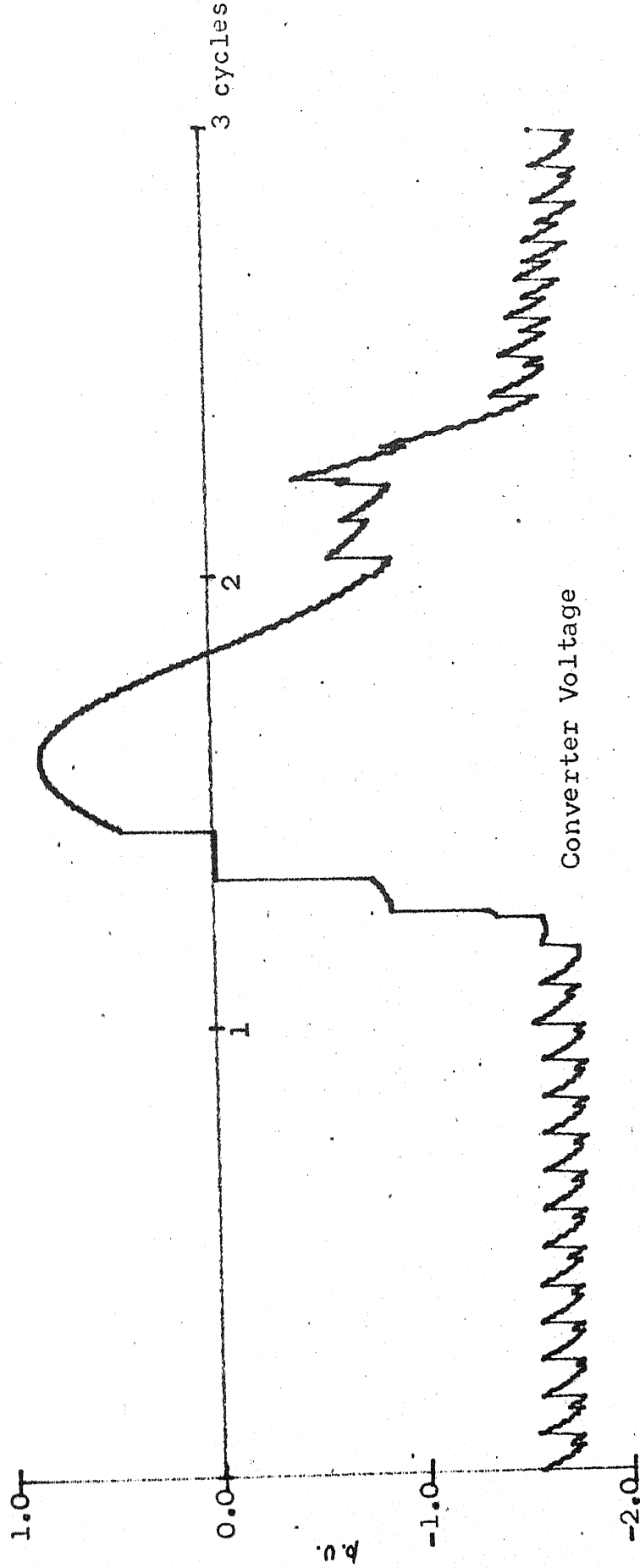


Fig. 3.5 COMMUTATION FAILURE DUE TO VOLTAGE DIP AT THE INVERTER TERMINAL

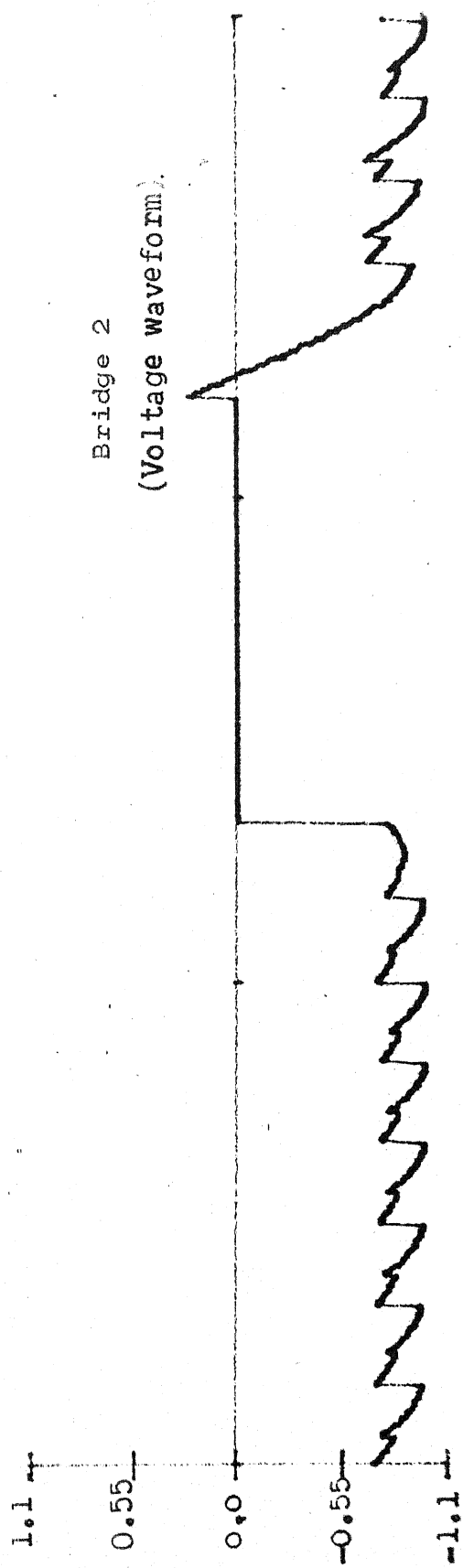
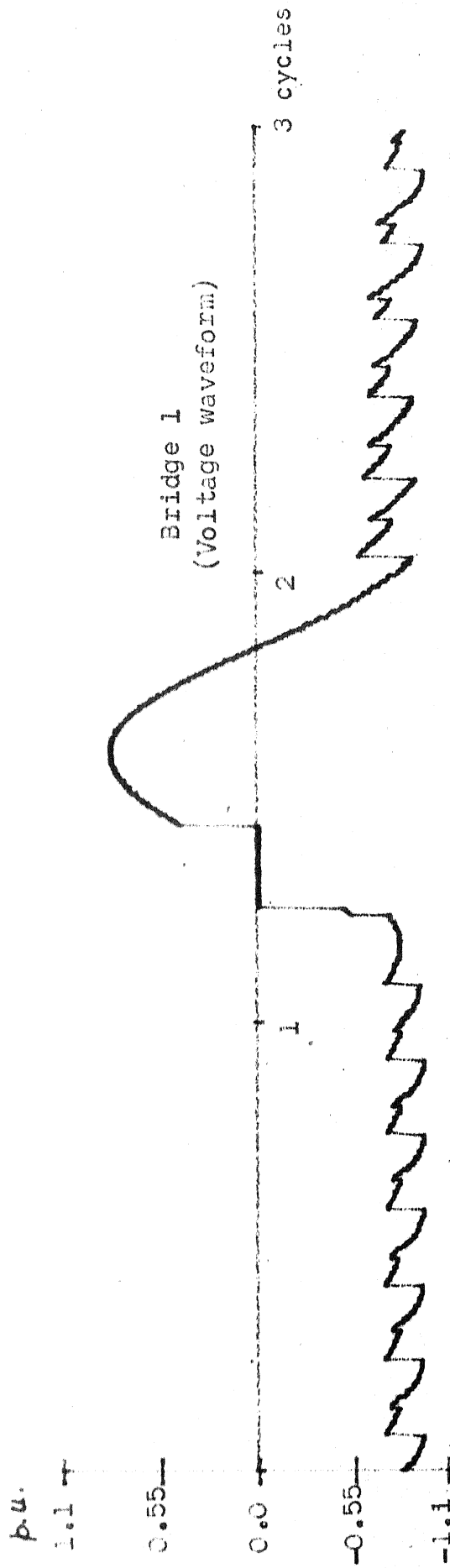


Fig. 3.6 SHOWS THE COMMUTATION FAILURE IN THE BRIDGES (12 PULSE CONVERTER)

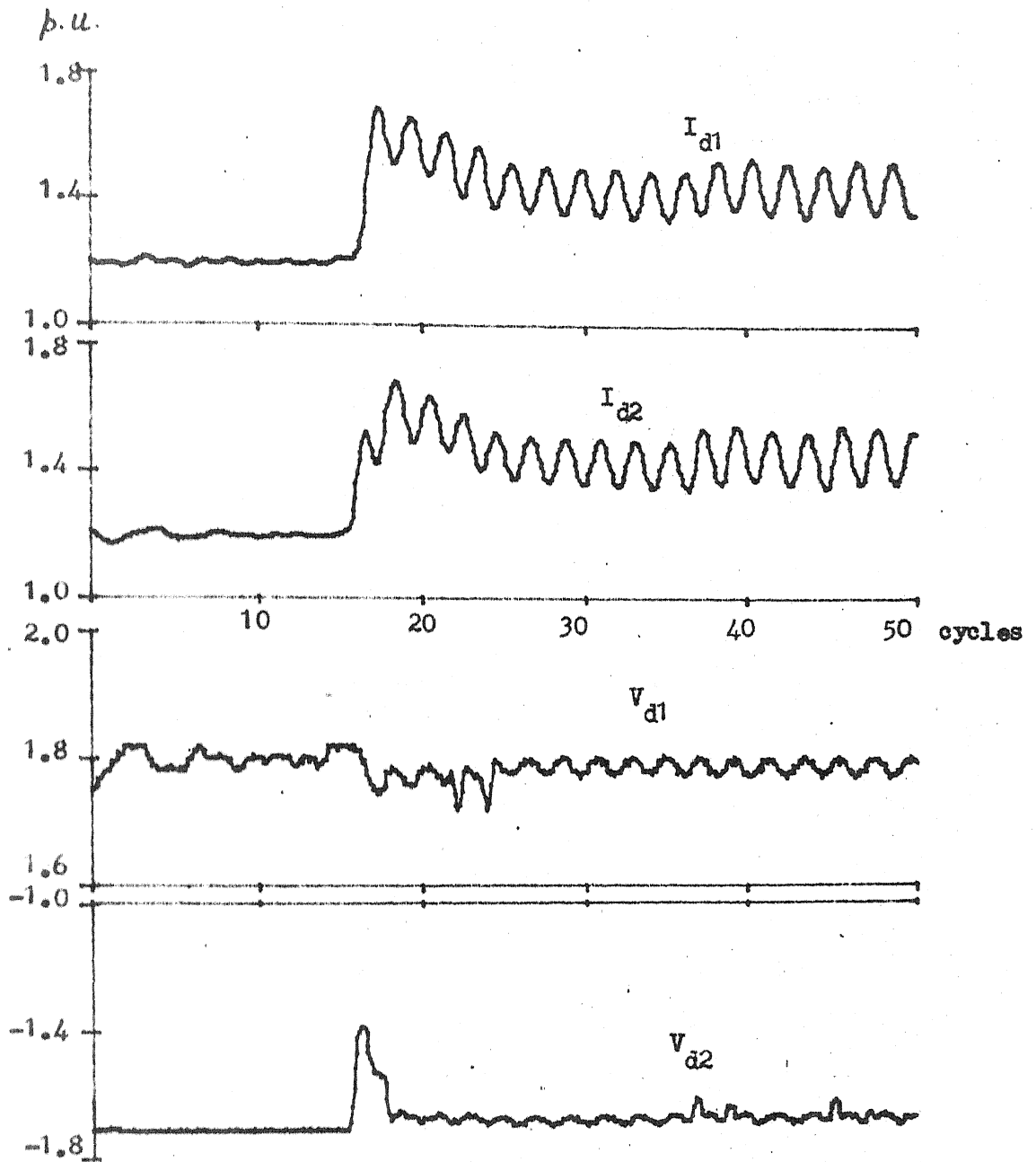
The system response for the above cases are shown in Figs. 3.7 to 3.10. All the above figures show the variation of average dc current and dc voltages over 50 cycles of simulation. The averaging is done for every 30 degrees. In all the cases, the disturbance is initiated at the beginning of 15th cycle of the simulation.

Discussion

The responses illustrate the controller action following the step change in the current reference setting. For case (i), while with IPC firing scheme the oscillations are observed in dc current and voltage, with EPC firing scheme these oscillations are negligible. With the increase in the magnitude of the step change in the current reference setting (case ii) the oscillations in the dc current and voltage are noticeable with both IPC and EPC firing schemes. In the cases studied EPC appears to be more effective than IPC firing scheme.

3.4 CONCLUSION

In this chapter, a computer program developed for the dynamic digital simulation of HVDC system is described. The program employs both the individual phase control and equidistant pulse control firing schemes for converter control.

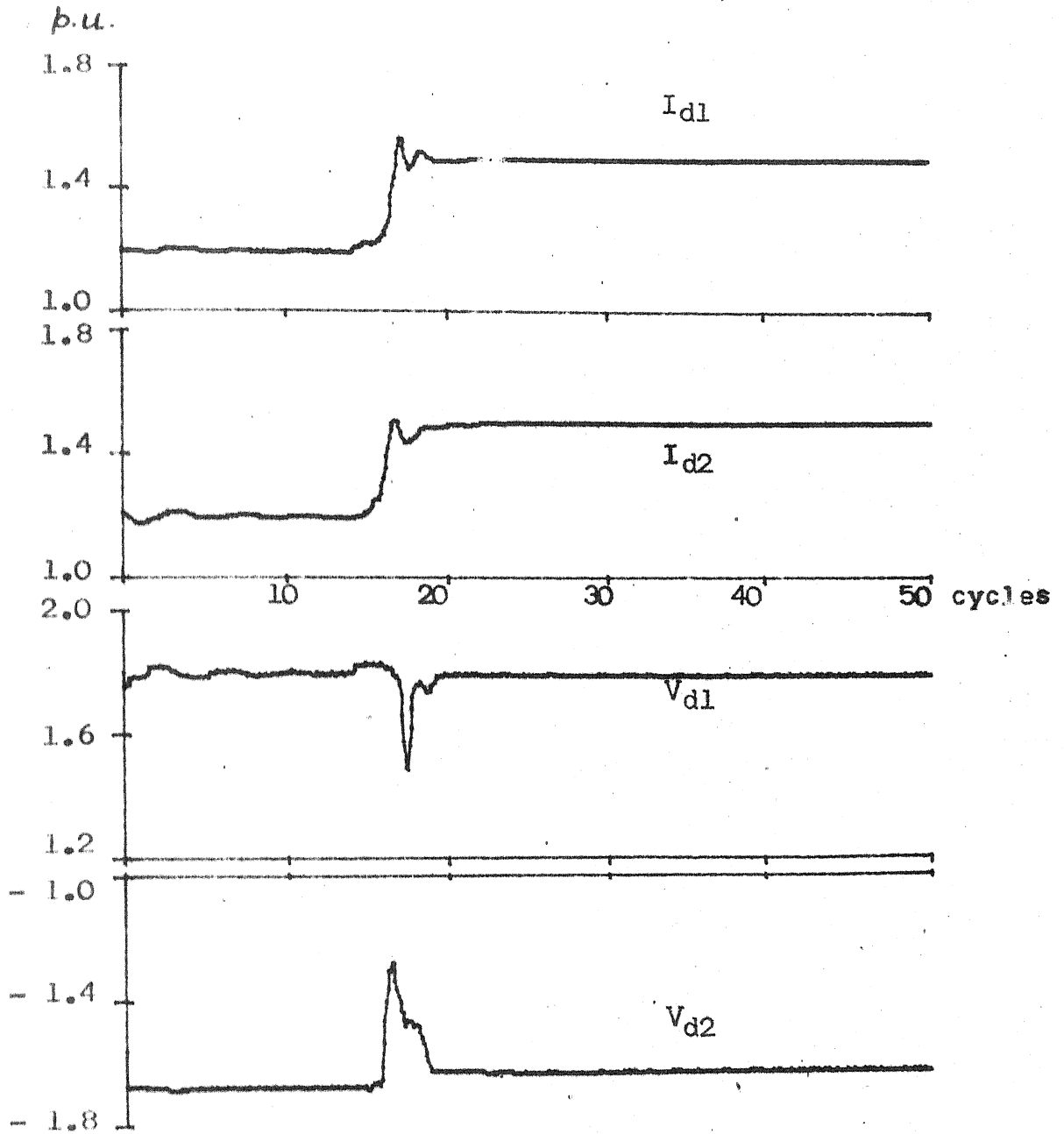


I_{Ref1} : 1.2 to 1.5

I_{ref2} : 1.1 to 1.4

IPC at both the terminals

Fig. 3.7 CASE A(1)



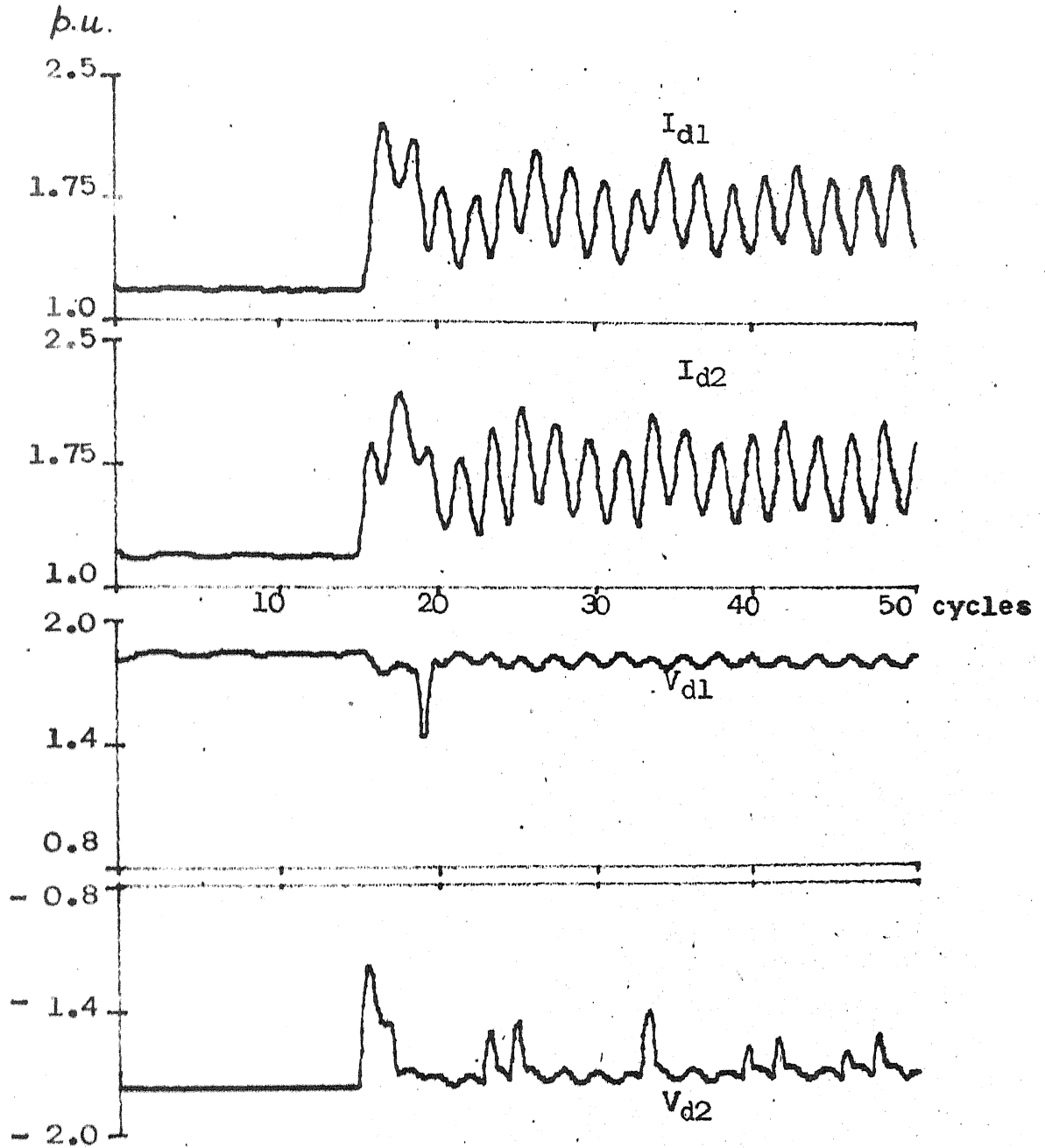
I_{ref1} : 1.2 to 1.5

I_{ref2} : 1.1 to 1.4

EPC at rectifier

IPC at inverter

Fig. 3.8 CASE B(1)



I_{ref1} : 1.2 to 1.75

I_{ref2} : 1.1 to 1.65

IPC at both the terminals

Fig. 3.9 CASE A(ii)

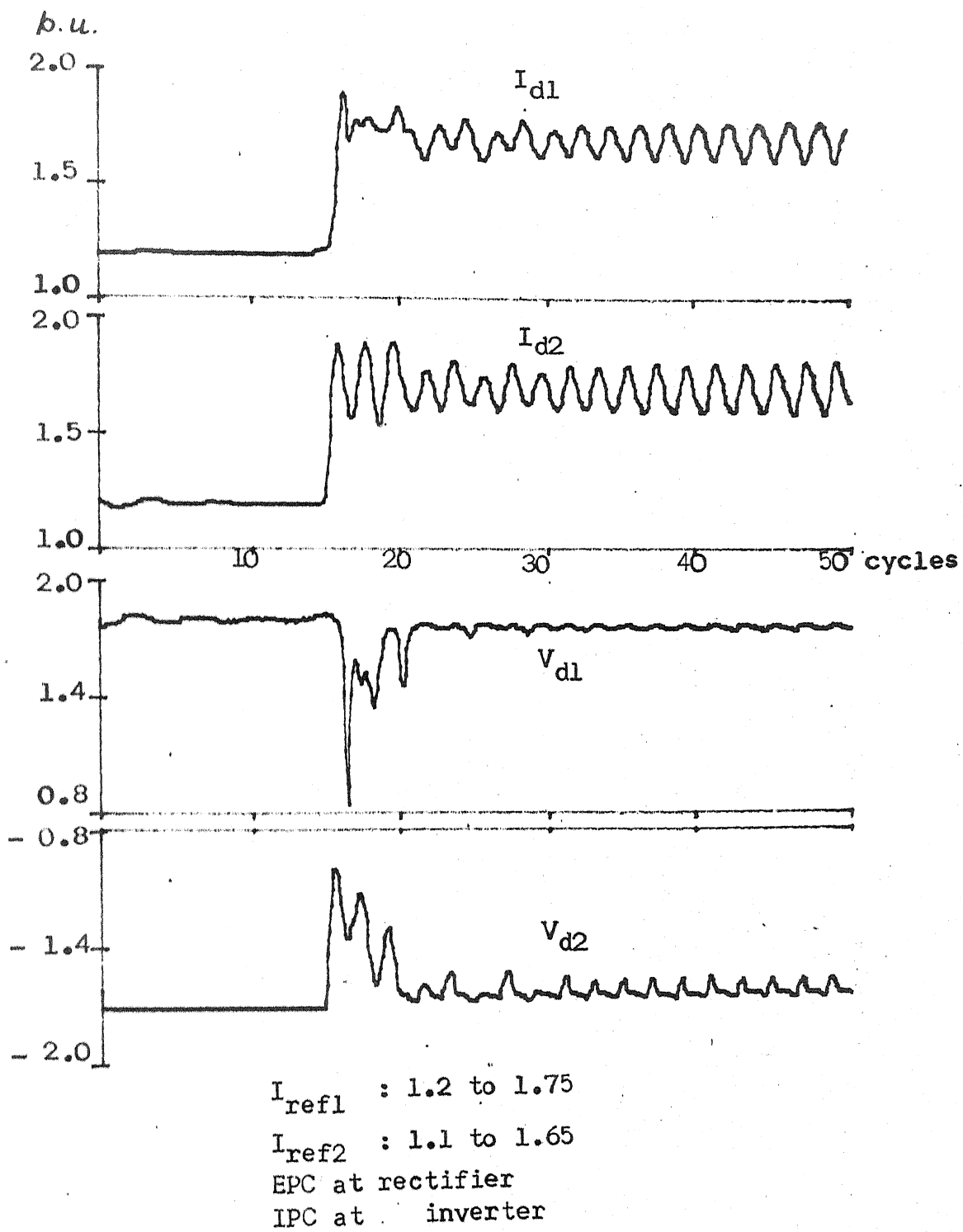


Fig. 3.10 CASE B(ii)

Results of the various test simulations for 2 terminal HVDC system are presented primarily to illustrate the capability of the program and they clearly show the need for proper design of controllers whose performance is influenced by the system parameters.

CHAPTER 4

SIMULATION OF HVDC LINK WITH AC REPRESENTATION

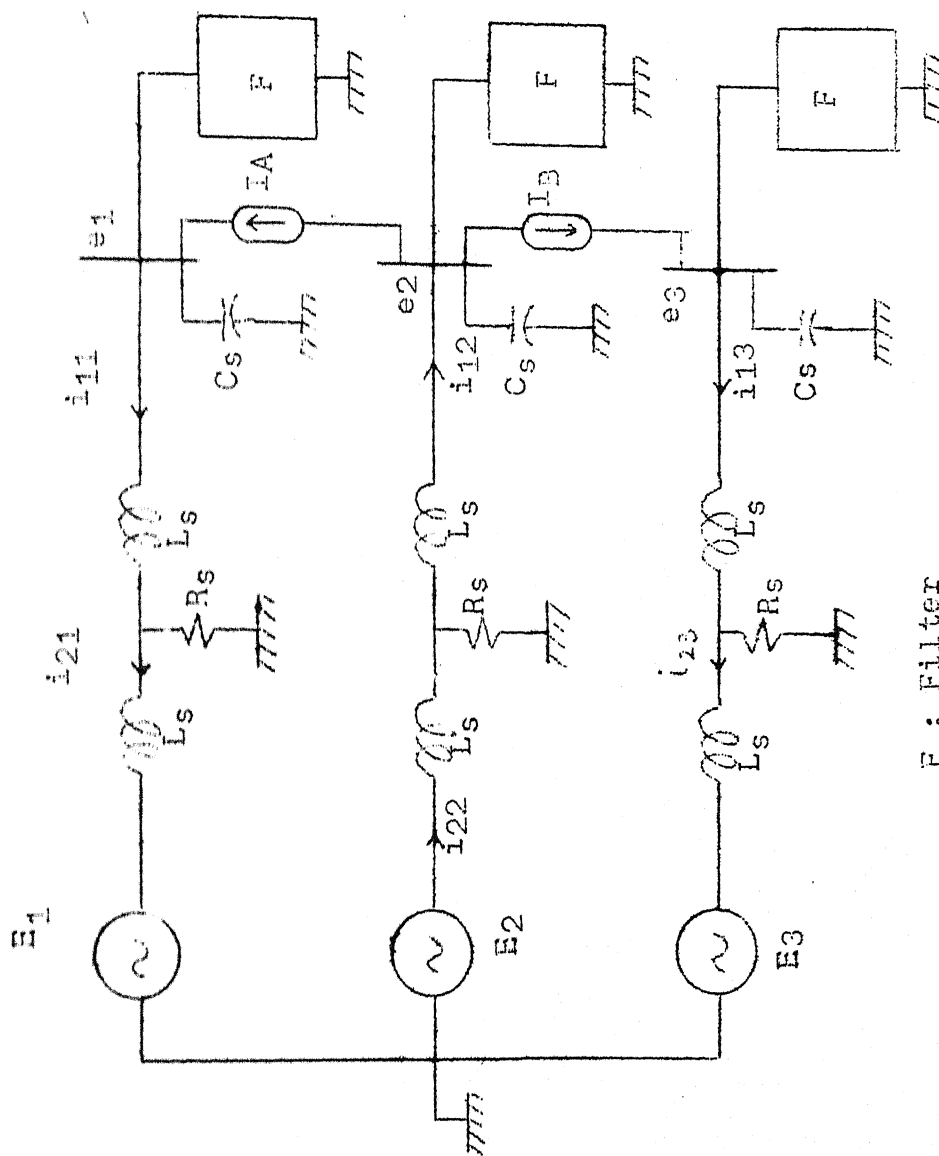
4.1 INTRODUCTION

Detailed representation of the ac system and harmonic filters is required to investigate the effect of interaction between ac and dc system dynamics on the system behaviour. The performance of the HVDC system, particularly under transient conditions deteriorates drastically when the ac system short circuit ratio (SCR) at the converter bus is low.

A state space model of the ac system alongwith the harmonic filters has been formulated. Both steady state and transient studies have been carried out with detailed ac representation, after suitably augmenting the previous program described in the previous chapter.

4.2 AC SYSTEM MODEL

The schematic 3 ϕ representation of the ac system and harmonic filters feeding a particular converter is shown in Fig. 4.1. The ac system is represented by an ideal source voltage (E_j) behind a T equivalent circuit for each phase of the ac network. The inductance (L_s) and resistance (R_s) at the fundamental frequency are determined from the knowledge of SCR at the converter ac terminal and impedance



F : Filter

Fig. 4.1 AC SYSTEM REPRESENTATION

angle. R_s represents the effect of damping due to loads within the ac system. The shunt capacitance (C_s) is determined from the reactive power requirement of the converter. The effect of the converter is represented as current sources feeding into the ac network (I_A, I_B).

The current through inductors in the links and voltages across capacitors in the tree of the graph are chosen as the state variables to define the system state at any given time. The generalised state equation of the ac system will be of the form

$$\dot{x} = Ax + Bu \quad (4.1)$$

where u is the input, x is the state vector and A and B are constant matrices. The ac system state and output equations are given in the Appendix B.

4.3 INTERFACING THE CONVERTER AND AC SYSTEM

Power from the ac bus is fed to the bridges of the 12-pulse converter through two transformers each having an off-nominal tap setting (a). One transformer has wye-wye connection where as the other has a delta-wye connection to obtain the desired 30 degrees phase difference between the two sets of voltages. The voltages and currents on the two sides of the wye-wye connected transformer are related as

$$ae_1 = e_{as}^Y ; \quad ae_2 = e_{bs}^Y ; \quad ae_3 = e_{cs}^Y$$

$$i_{ap}^Y = ai_9^Y ; \quad i_{cp}^Y = ai_7^Y$$

and the corresponding relations for the delta-wye connected transformer are,

$$e_{as}^\Delta = \frac{a}{\sqrt{3}} (e_1 - e_2)$$

$$e_{bs}^\Delta = \frac{a}{\sqrt{3}} (e_2 - e_3)$$

$$e_{cs}^\Delta = \frac{a}{\sqrt{3}} (e_3 - e_1)$$

$$i_{ap}^\Delta = \frac{a}{\sqrt{3}} (2i_9^\Delta + i_7^\Delta)$$

$$i_{cp}^\Delta = \frac{a}{\sqrt{3}} (2i_7^\Delta + i_9^\Delta)$$

The schematic diagram illustrating the interfacing of a converter and the ac system, is shown in Fig. 4.2. Here, I_A and I_B are defined as follows

$$I_A = i_{ap}^Y + i_{ap}^\Delta$$

$$I_B = i_{cp}^Y + i_{cp}^\Delta$$

The ac voltages e_{as}^Y , e_{bs}^Y , e_{cs}^Y , e_{as}^Δ , e_{bs}^Δ and e_{cs}^Δ are used in the converter model (refer Fig. 2.1). The ac currents (i_7^Y , i_7^Δ , i_9^Y and i_9^Δ) are obtained from the converter

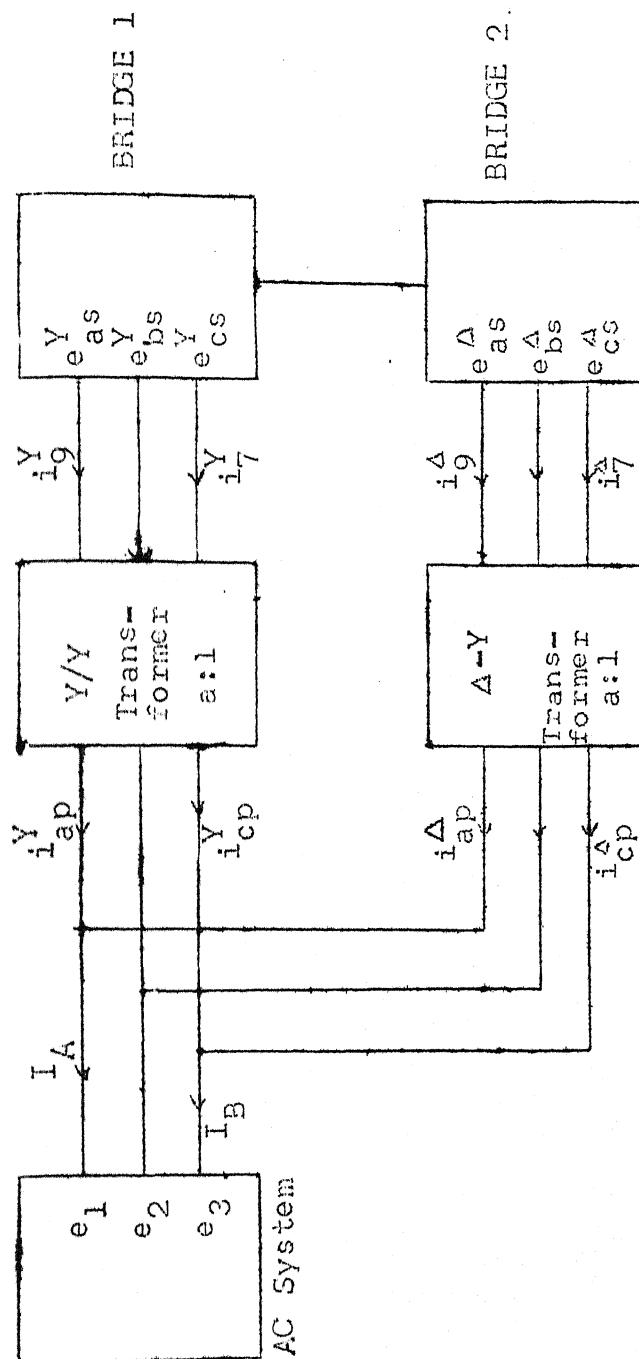


FIG. 4.2: INTERFACE BETWEEN AC SYSTEM AND CONVERTER MODEL

model. Since the program (described in the previous chapter) is developed on modular approach, it is augmented to include the ac system equations also. From the knowledge of the source currents (I_A and I_B), equations B.1 to B.7 are solved at each integration time step to determine the voltages e_1 , e_2 and e_3 (i.e., e_j , refer Appendix B). This in turn establishes transformer secondary voltages (Fig. 4.2) which are used subsequently for the solution of the converter dynamic equations. The transformer tap is assumed fixed at the initial operating value determined from the load flow calculations.

4.4 TEST SIMULATION

The program capability is illustrated through simulation of a single terminal and two terminal HVDC system shown respectively in Figs. 4.3 and 3.2. In the AC system configuration shown in Fig. 4.1, each of the block marked 'F' contains 4 series tuned filters (i.e. 5th, 7th, 11th, and 13th harmonic filters) and a second order high pass filter (refer Figs. B.1 and B.2 for filter configuration). The detail system parameters and operating conditions are given in Appendix C.

4.4.1 Steady State Response

The steady state waveforms for a single converter, acting as a rectifier, with ac system of SCR equal to 15 and

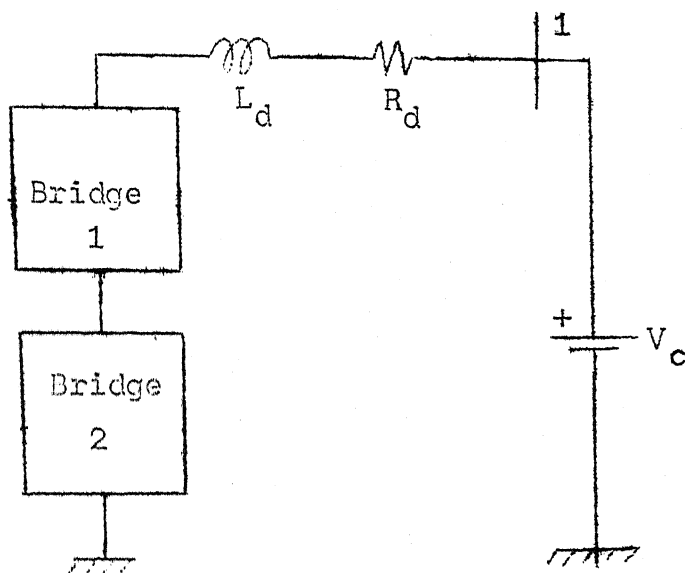


Fig. 4.3 SINGLE TERMINAL HVDC SYSTEM
FEEDING A CONSTANT VOLTAGE
SOURCE

with filters included (operating conditions A) assuming IPC and EPC firing schemes, are shown in Figs. 4.4 and 4.5 respectively. From Fig. 4.4 it is observed that the firing instants are not equally spaced, but not so for the case of EPC firing scheme shown in Fig. 4.5. For the same system without filters (operating conditions B) the steady state waveforms assuming IPC and EPC schemes are shown in Figs. 4.6 and 4.7 respectively. The difference in steady state waveforms, with and without filters, is quite significant for IPC firing scheme but not for EPC scheme. Thus, it is evident, due to unequally spaced firing instants, IPC has an inherent tendency to enhance harmonic generation.

4.4.2 Effect of Harmonic Filters

The effect of harmonic filters can be seen from the test simulation results given in the Figs. 4.8 to 4.11. The difference in the ac currents and ac voltage of phase A with and without filters assuming IPC firing scheme are shown in Figs. 4.8 and 4.9 respectively. The above waveforms with EPC firing scheme, are shown in Figs. 4.10 and 4.11. When EPC is used, hardly any disparity can be observed between the ac injected currents, I_A with and without filters. The above Figs. 4.10 and 4.11 also depict the nature of the injected current.

CENTRAL LIBRARY

Acc. No. A 8:181

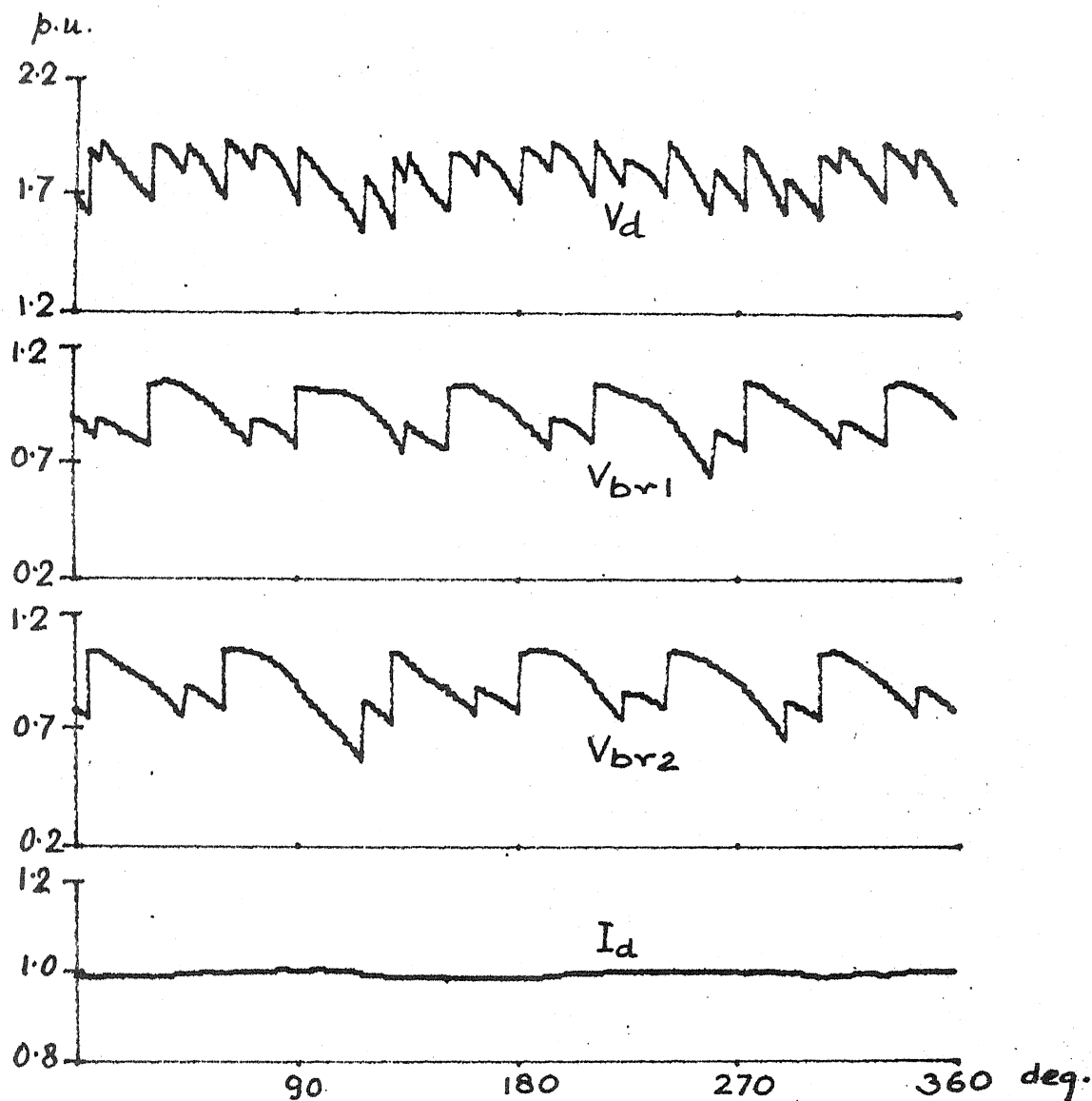


FIG. 4.4 STEADY STATE WAVEFORMS FOR SINGLE
 TERMINAL SYSTEM WITH AC SYSTEM(SCR=15)
 AND FILTERS
 IPC FIRING SCHEME IS EMPLOYED

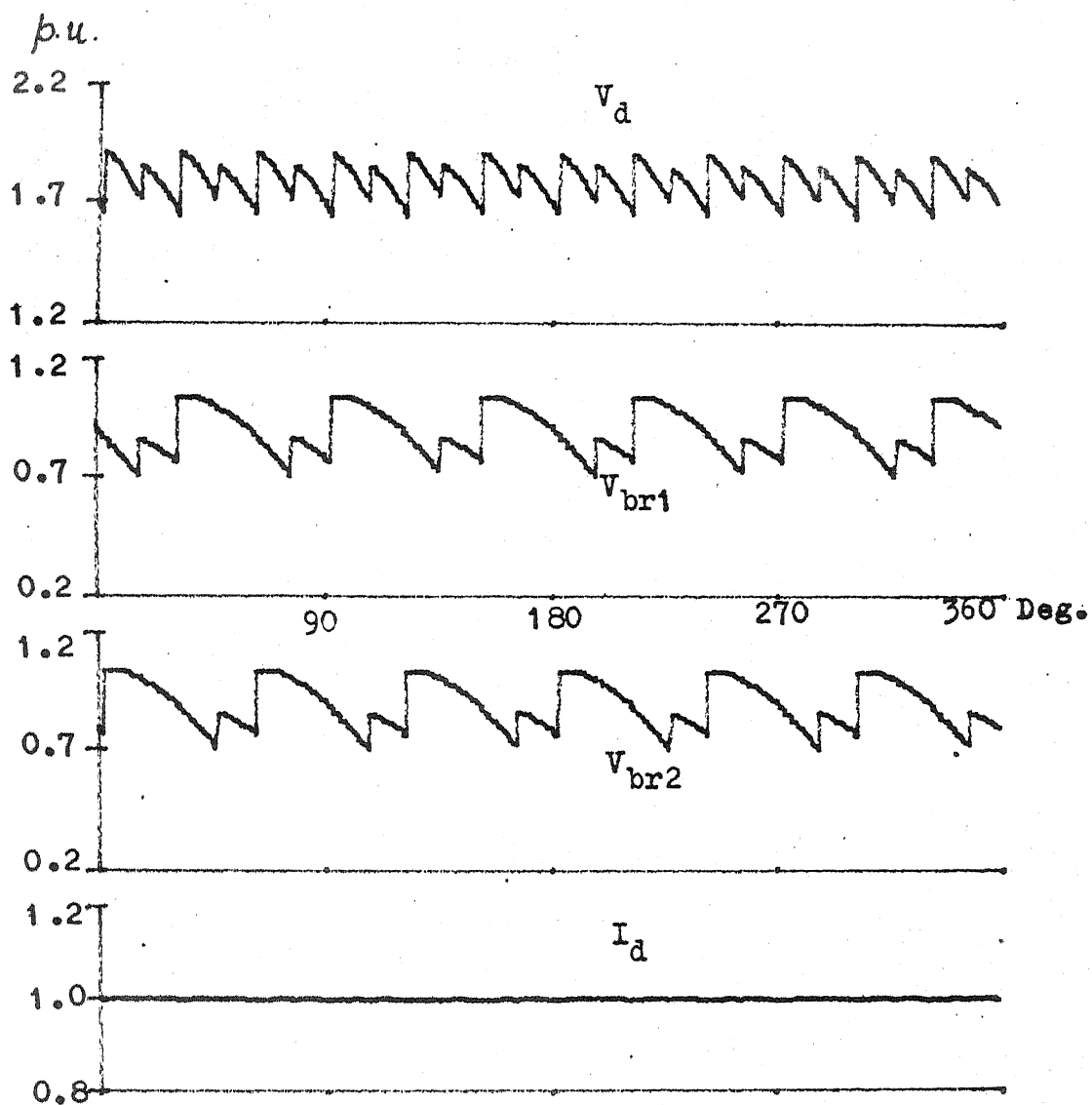


Fig. 4.5 STEADY STATE WAVEFORMS FOR A SINGLE
TERMINAL SYSTEM WITH AC SYSTEM
(SCR=15) AND FILTERS, EPC FIRING SCHEME

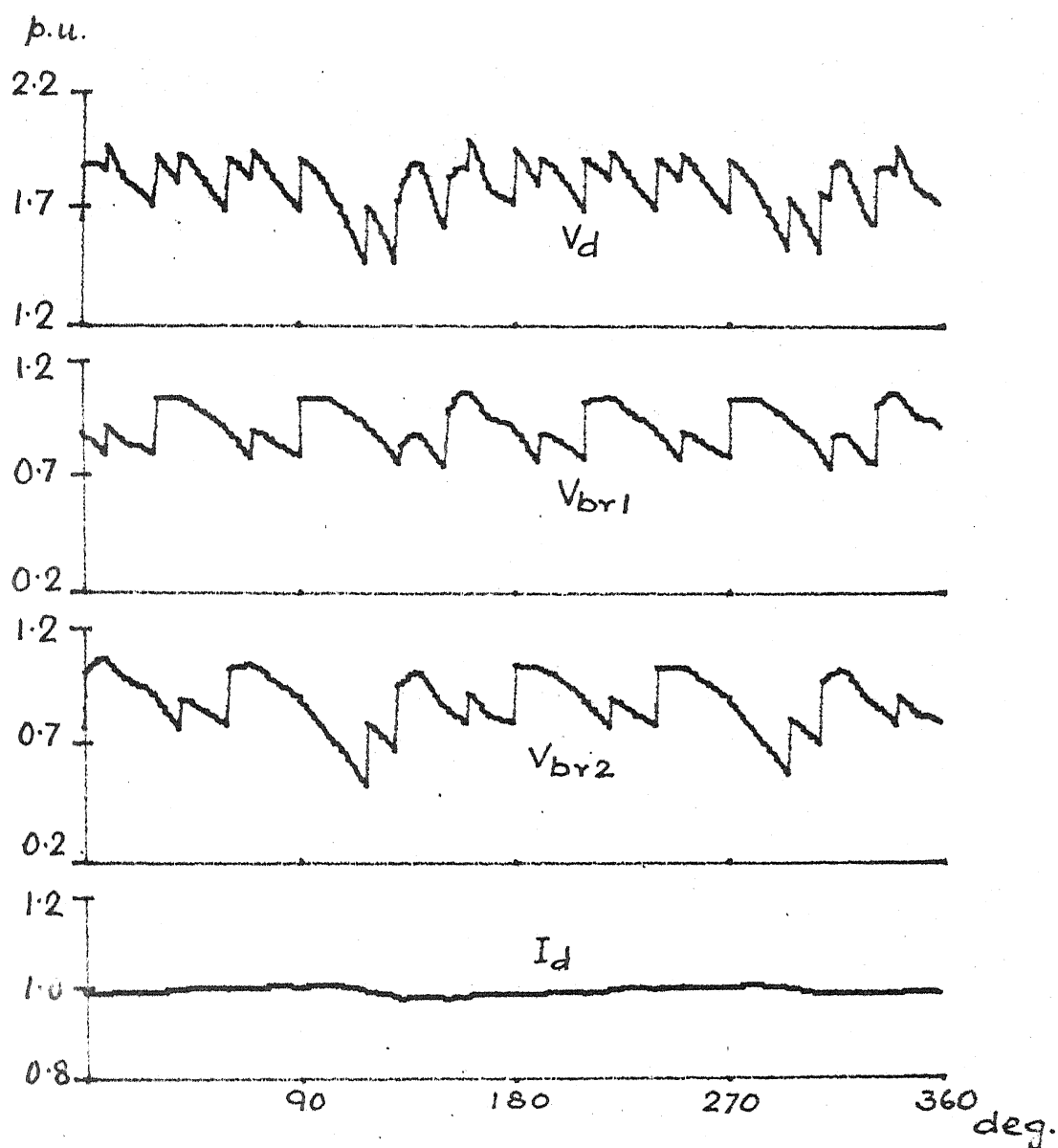


Fig. 4.6 STEADY STATE WAVEFORMS FOR SINGLE
TERMINAL SYSTEM WITH AC SYSTEM
(SCR= 15) AND WITHOUT FILTERS,
IPC FIRING SCHEME

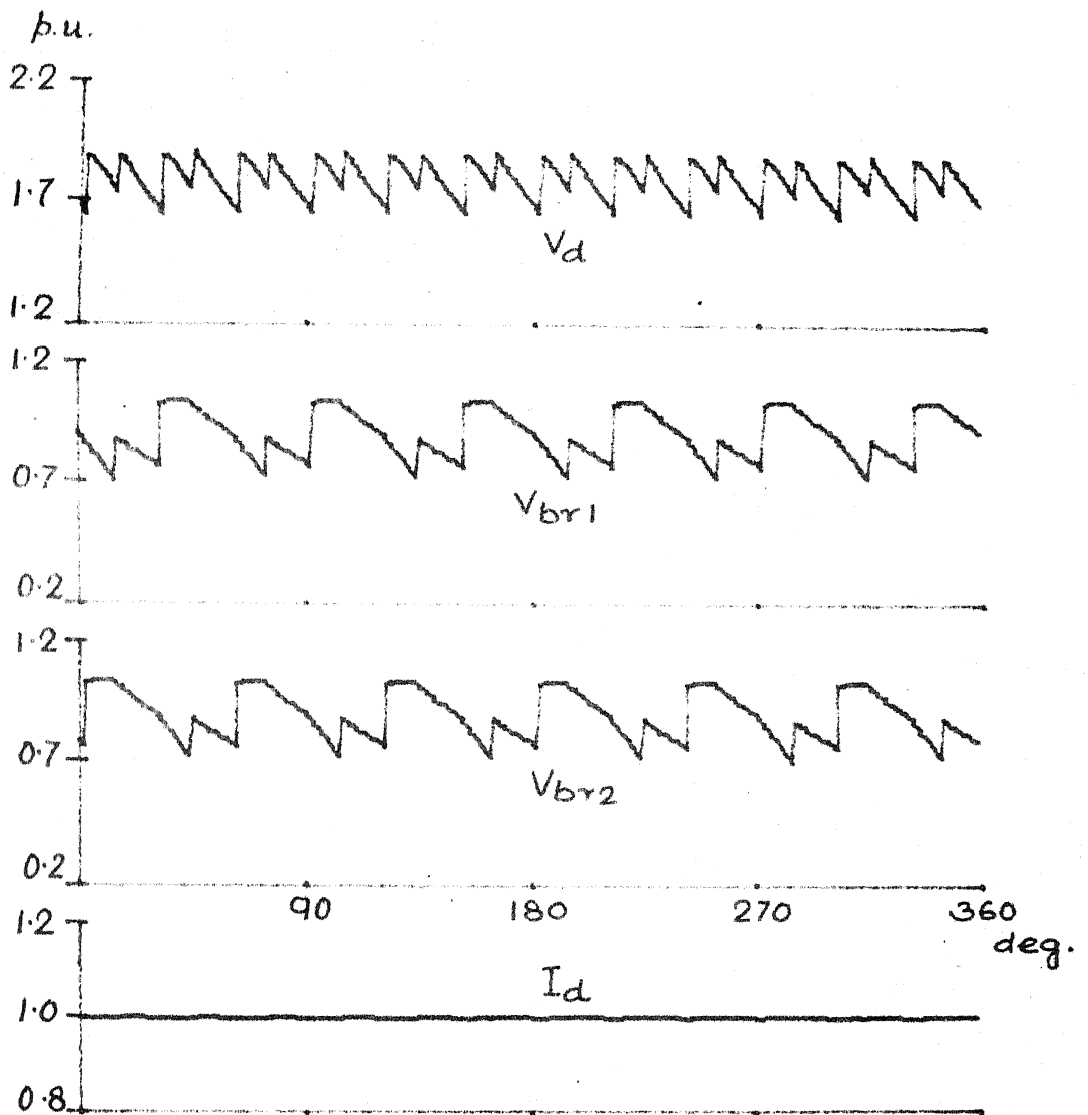
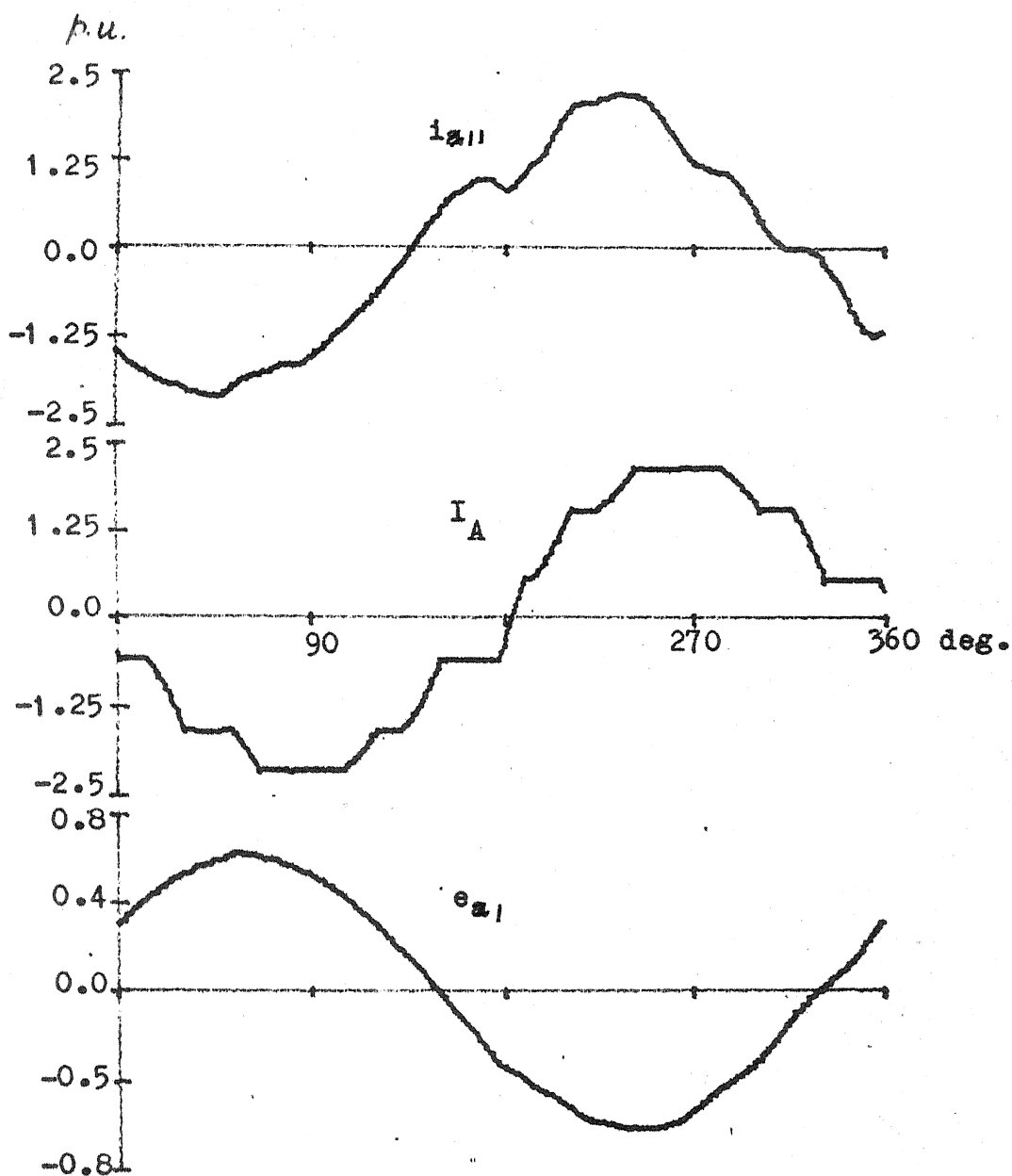
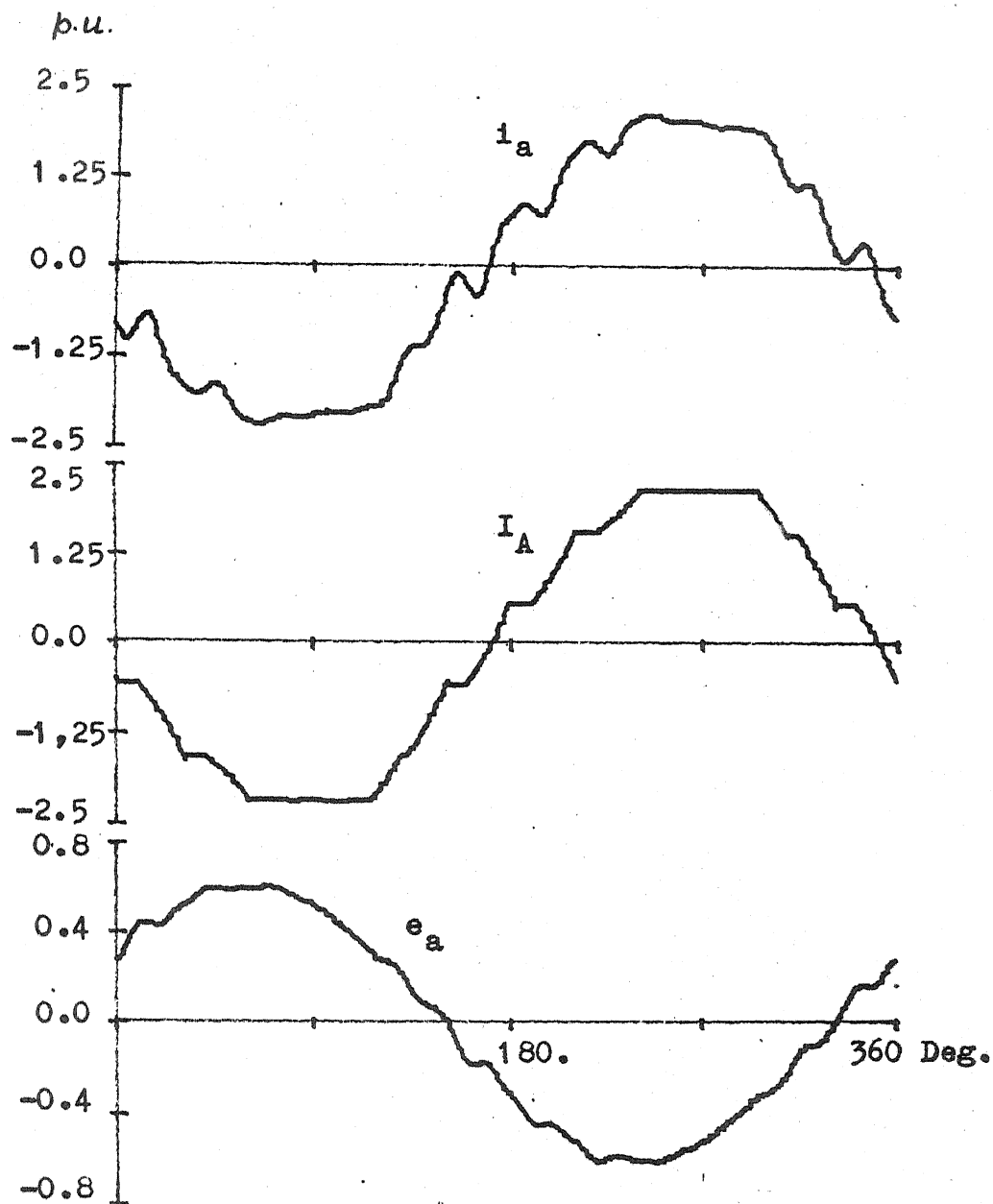


Fig. 4.7 STEADY STATE WAVEFORMS FOR SINGLE
 TERMINAL SYSTEM WITH AC SYSTEM
 (SCR= 15) AND WITHOUT FILTERS,
 EPC FIRING SCHEME.



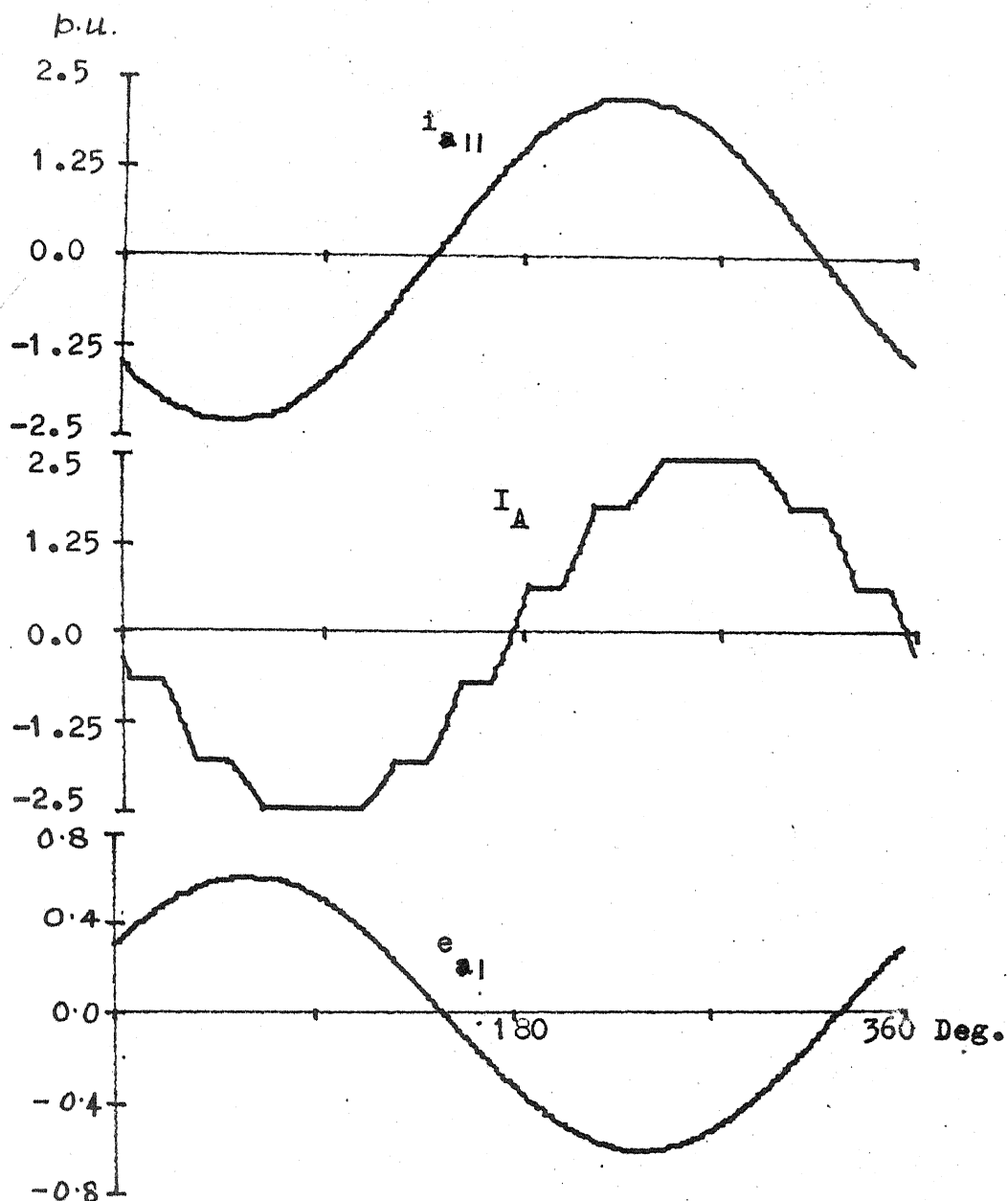
AC voltage and current waveforms of phase A,
 SCR = 15, IPC firing scheme with filters,
 and injected current I_A

Fig. 4.8 AC VOLTAGE AND CURRENT WAVEFORMS
 (IPC and filter)



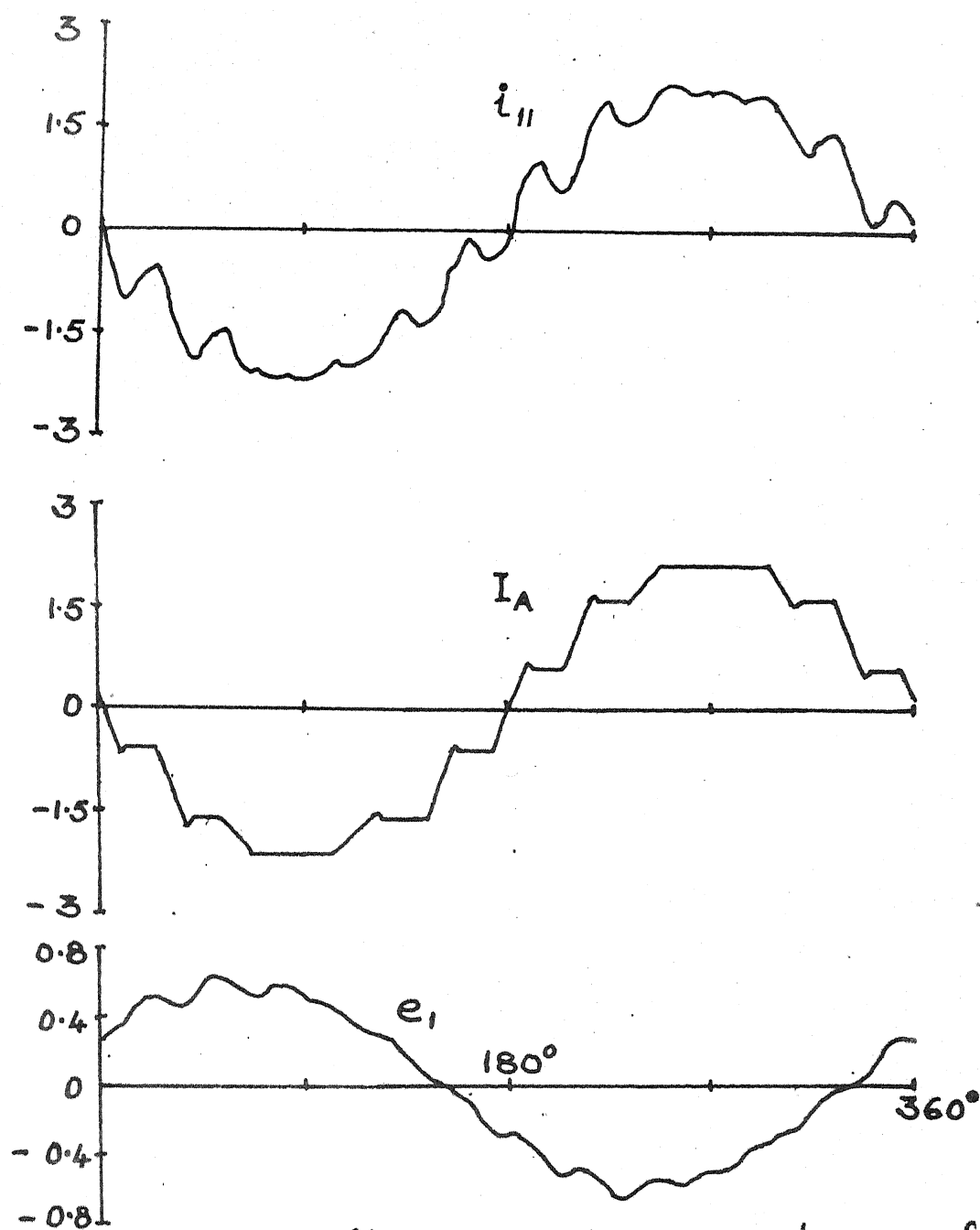
AC voltage and current waveforms of phase A, SCR =15, IPC firing scheme, without filters and injected current I_A

Fig. 4.9 AC VOLTAGE AND CURRENT WAVEFORMS (IPC ~~on~~ without filter)



AC voltage and current waveforms of Phase A,
EPC firing scheme, SCR =15, with filters
and injected current I_A

Fig. 4.10 AC VOLTAGE AND CURRENT WAVEFORMS
(EPC and filter)



Ac voltage and current waveforms of phase A, EPC firing scheme, without filter ($SCR=15$) and injected current I_A

Fig. 4.11 AC VOLTAGE & CURRENT WAVEFORMS (EPC without filter)

Discussion

The steady state responses, for a single converter system, show that the filters are necessary if IPC firing scheme is employed at the rectifier. Thus, the distortion in the ac voltage has least effect on EPC firing scheme, whereas IPC is more prone to introduce harmonics as its firing pulse generation is based on the zero crossing of the commutation voltages. Comparison of the responses given in Figs. 4.12 and 4.13 (assuming IPC and EPC schemes respectively) shows that IPC firing scheme introduces low frequency oscillation in the dc voltages but EPC scheme does not.

4.4.3 Transient Response

Transient responses are determined for a 2 terminal HVDC system where ac system representation is considered only at the inverter terminal. The disturbance chosen is the change in current reference setting to observe the system responses with IPC and EPC firing schemes when the inverter is feeding a strong and a weak ac system.

For 2 terminal HVDC system

A: with IPC firing schemes at both the terminals

i) $SCR = 15$ (operating condition C)

ii) $SCR = 7$ (operating condition D)

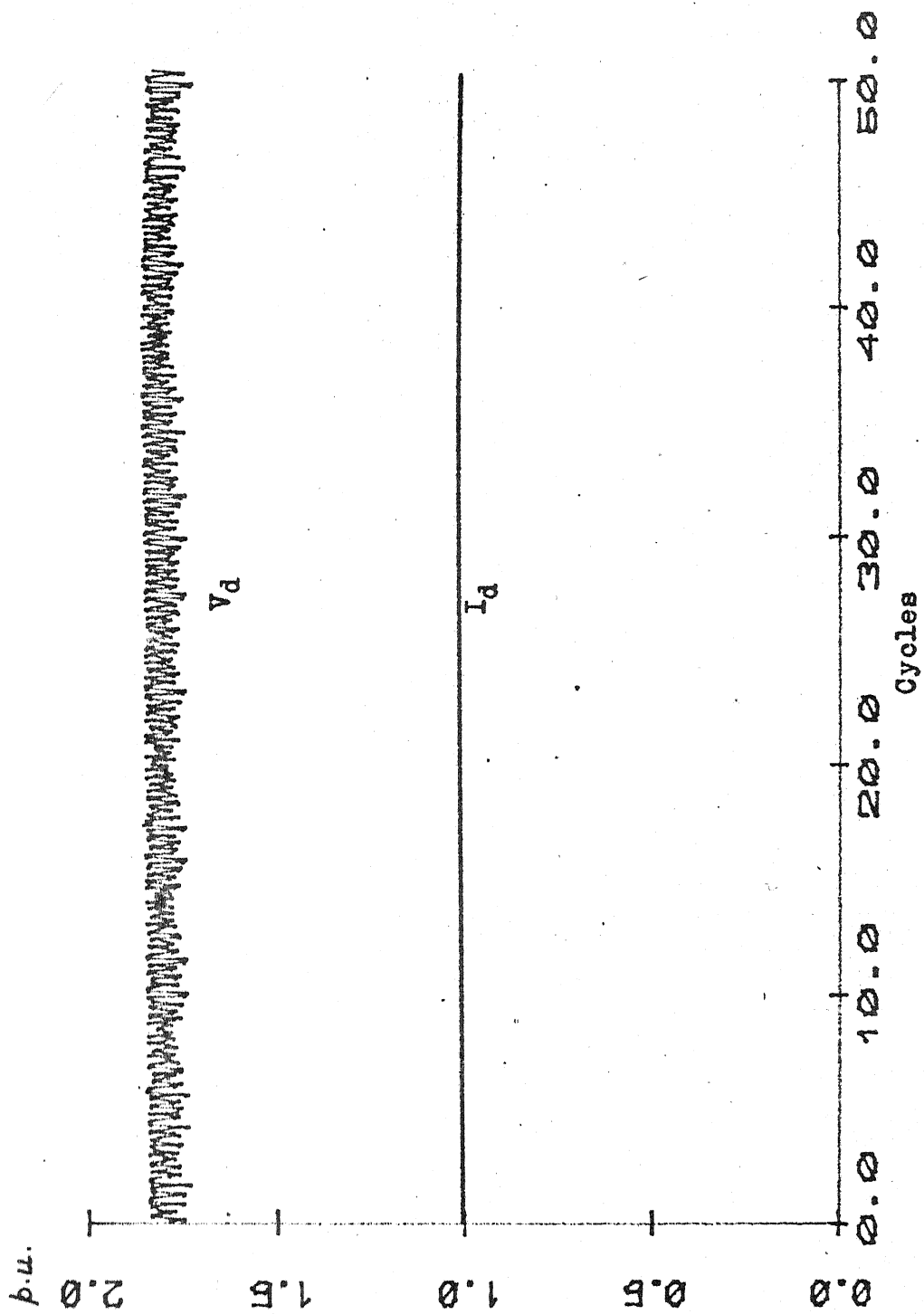


Fig. 4.12 VARIATION OF DC VOLTAGE AND CURRENT WITH FILTER
AND IPC FIRING SCHEME (SCR = 15)

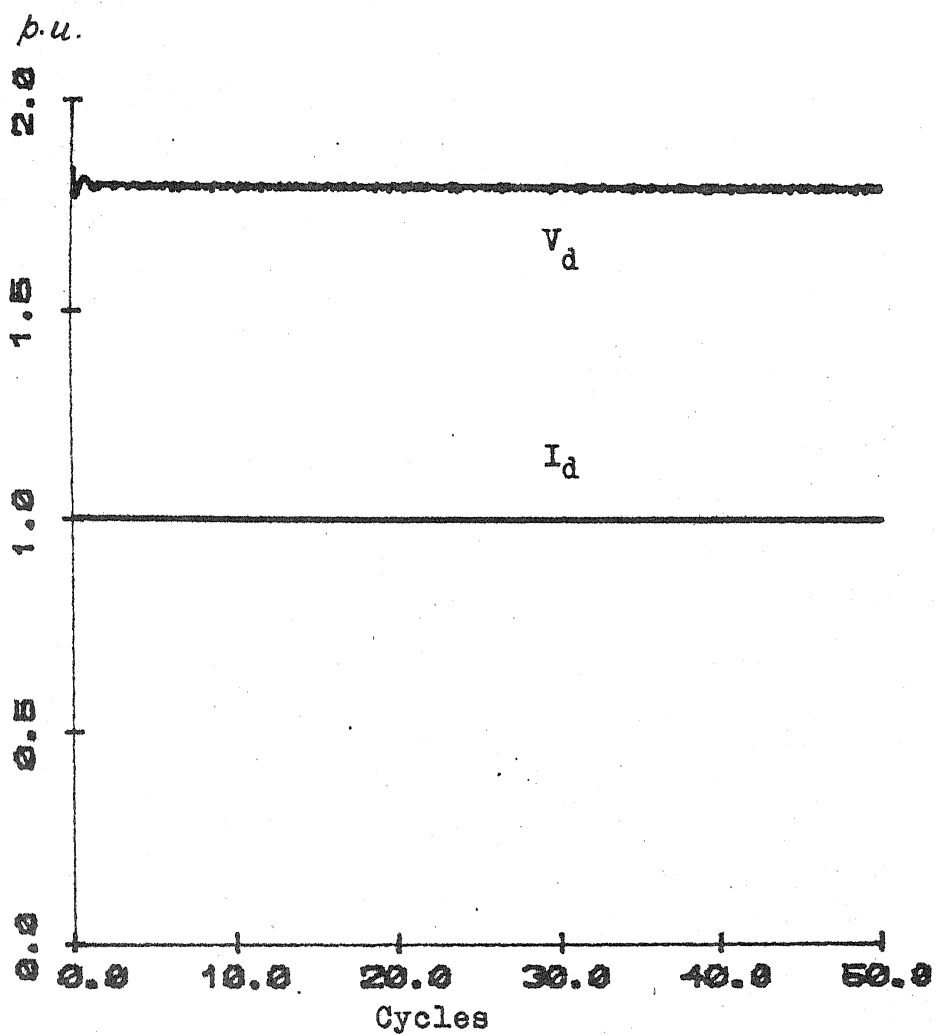


Fig. 4.13 VARIATION IN DC VOLTAGE AND CURRENT,
WITH FILTER AND EPC FIRING SCHEME
(SCR = 15)

B: with EPC at rectifier and IPC at inverter

i) SCR = 15 (operating condition C)

ii) SCR = 7 (operating condition D)

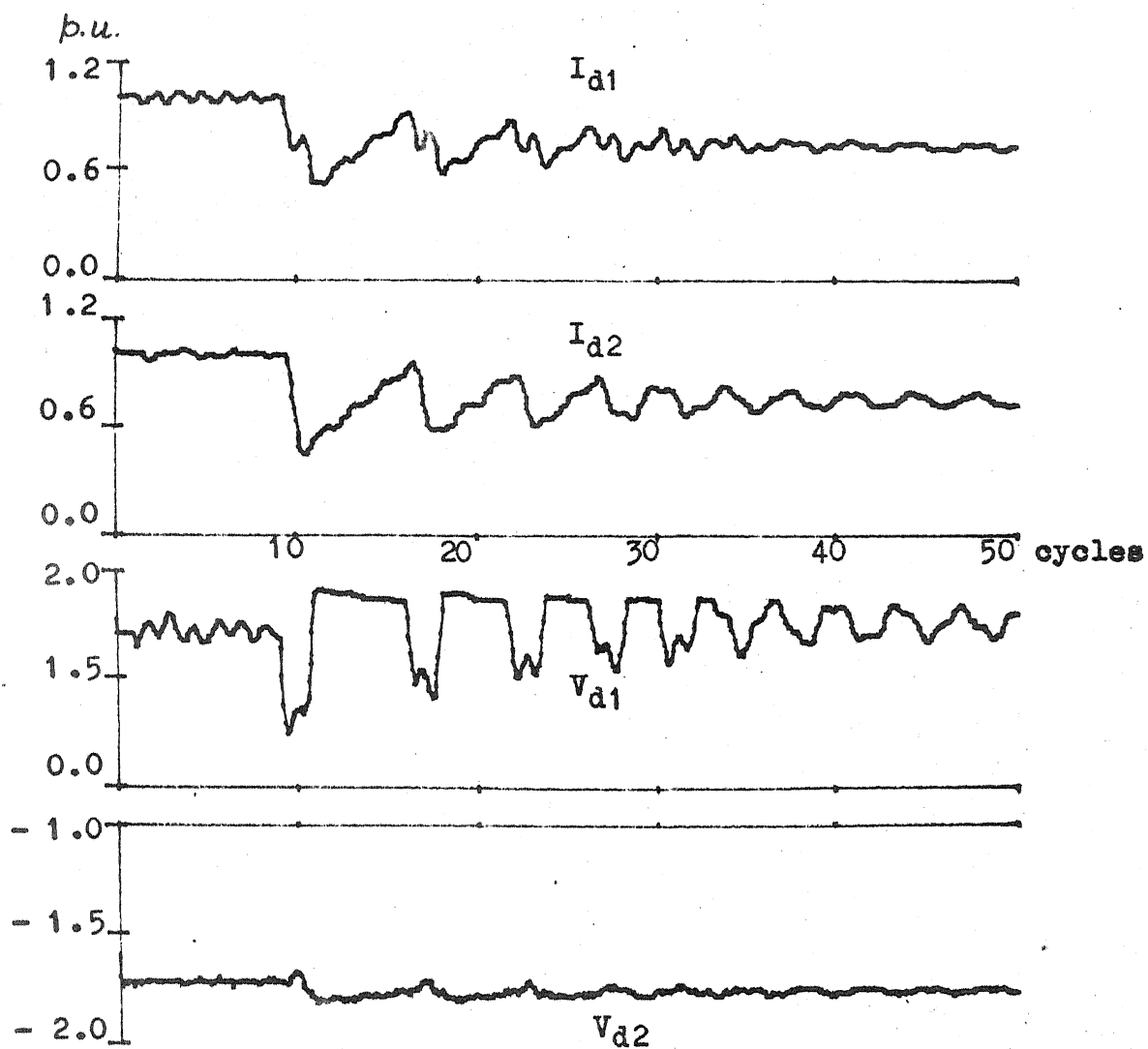
In both the cases the change in current reference setting I_{ref} is from 1.0 to 0.75 for terminal 1 and from 0.8 to 0.55 for terminal 2. The system responses for the above case are shown in Figs. 4.14 to 4.17. For all the cases the disturbance is initiated at the 10th cycle of the simulation.

Discussion

The transient responses for a two terminal system show that, following a change in the current reference setting, oscillations in dc current and voltage are present with IPC firing scheme at all terminals. It becomes quite significant if the converter is connected to ac system of low SCR (7). This undesirable influence of the ac system and filter parameters may perhaps be eliminated by proper controller design and use of control filters. With EPC at the rectifier alone, oscillation are found to reduce considerably and current settles down to the new setting in a reasonably short time.

4.5 CONCLUSION

In this chapter a state space model of the ac system including harmonic filters is described. This is interfaced with the converter model described in Chapter 2. The computer

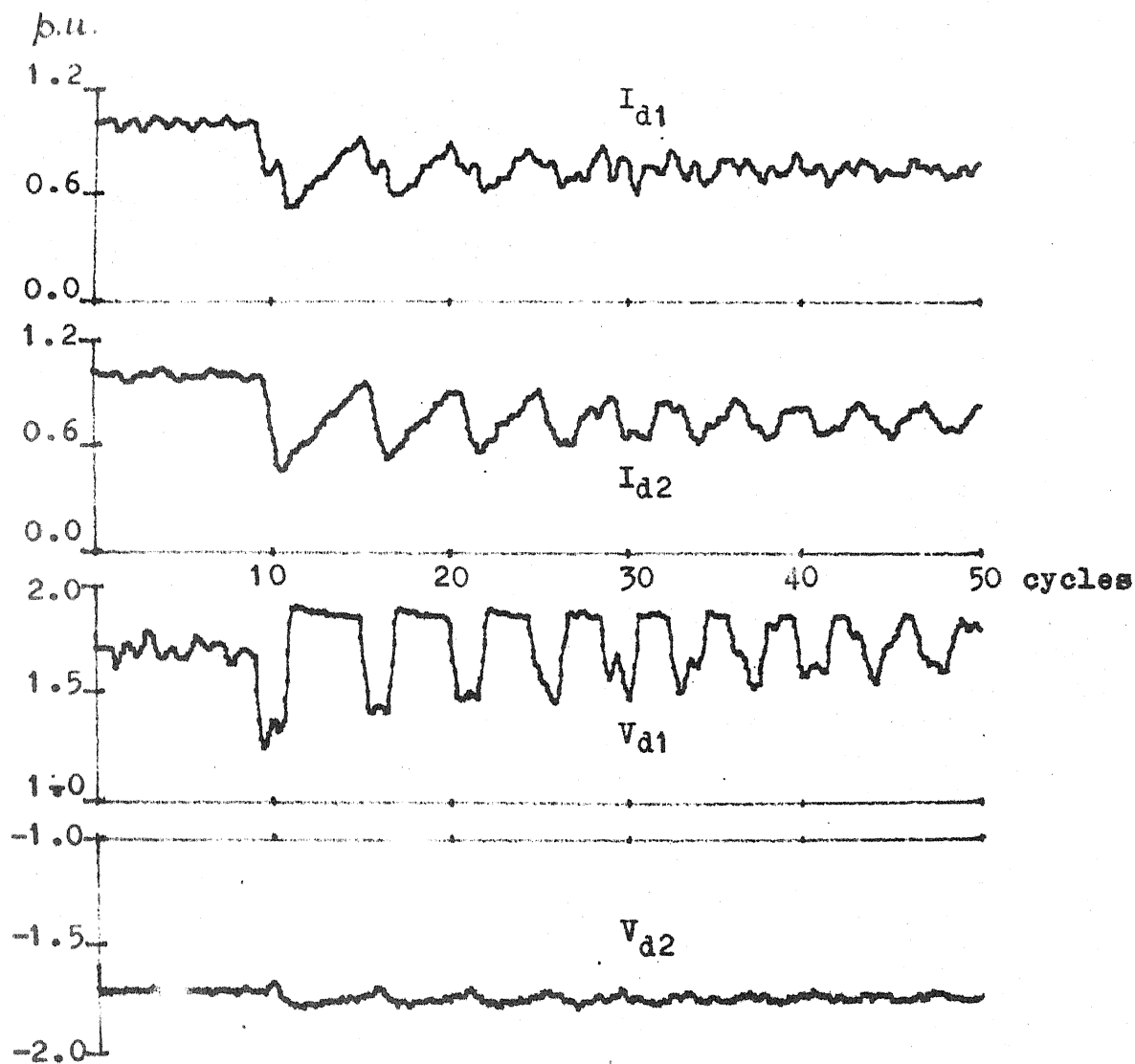


I_{ref1} : 1.0 to 0.75

I_{ref2} : 0.8 to 0.55

IPC at both the terminals, SCR = 15

Fig. 4.14 CASE A(i)



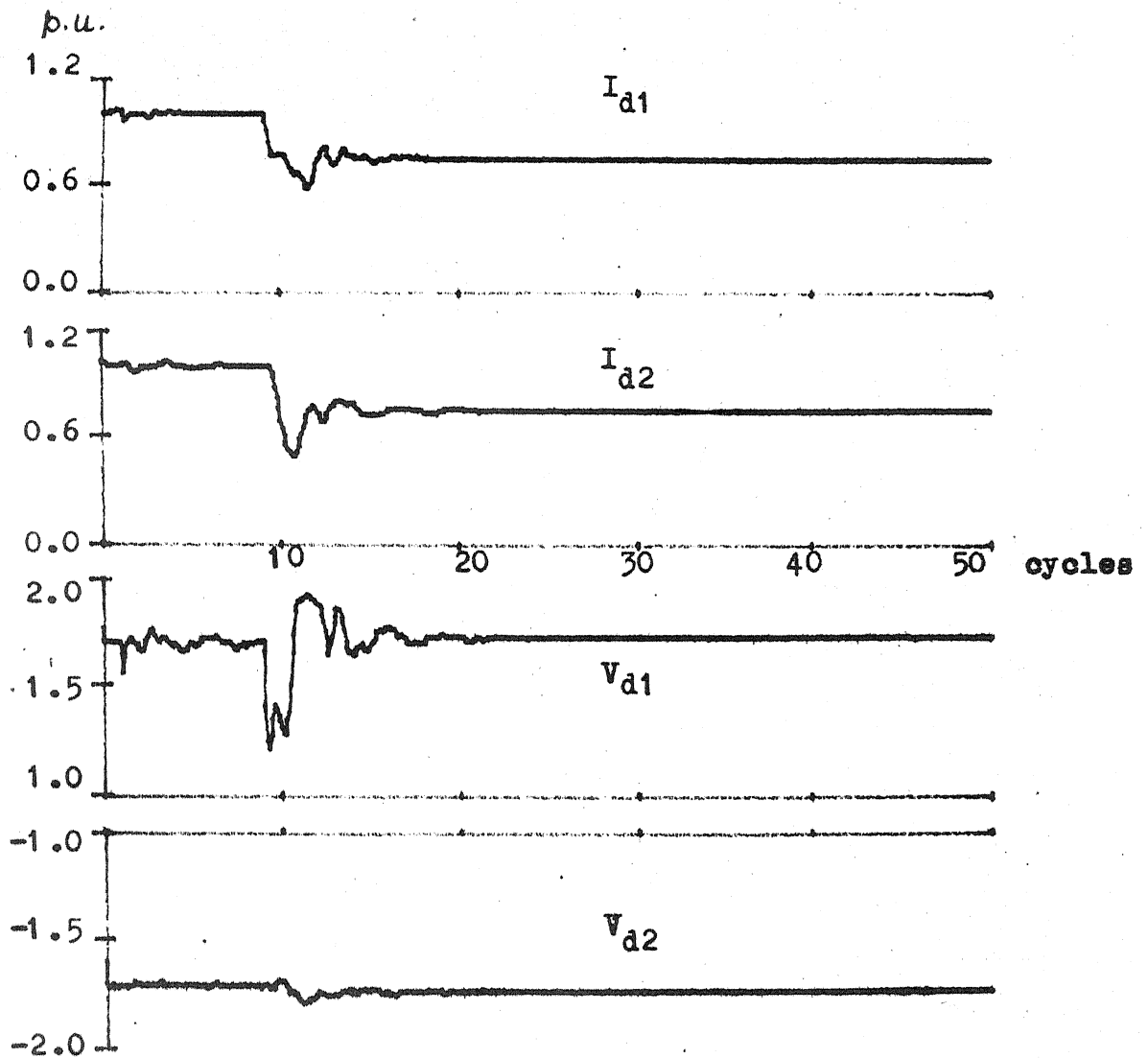
I_{ref1} : 1.0 to 0.75

I_{ref2} : 0.8 to 0.55

IPC at both the terminals

SCR = 7.0

Fig. 4.15 CASE A(ii)



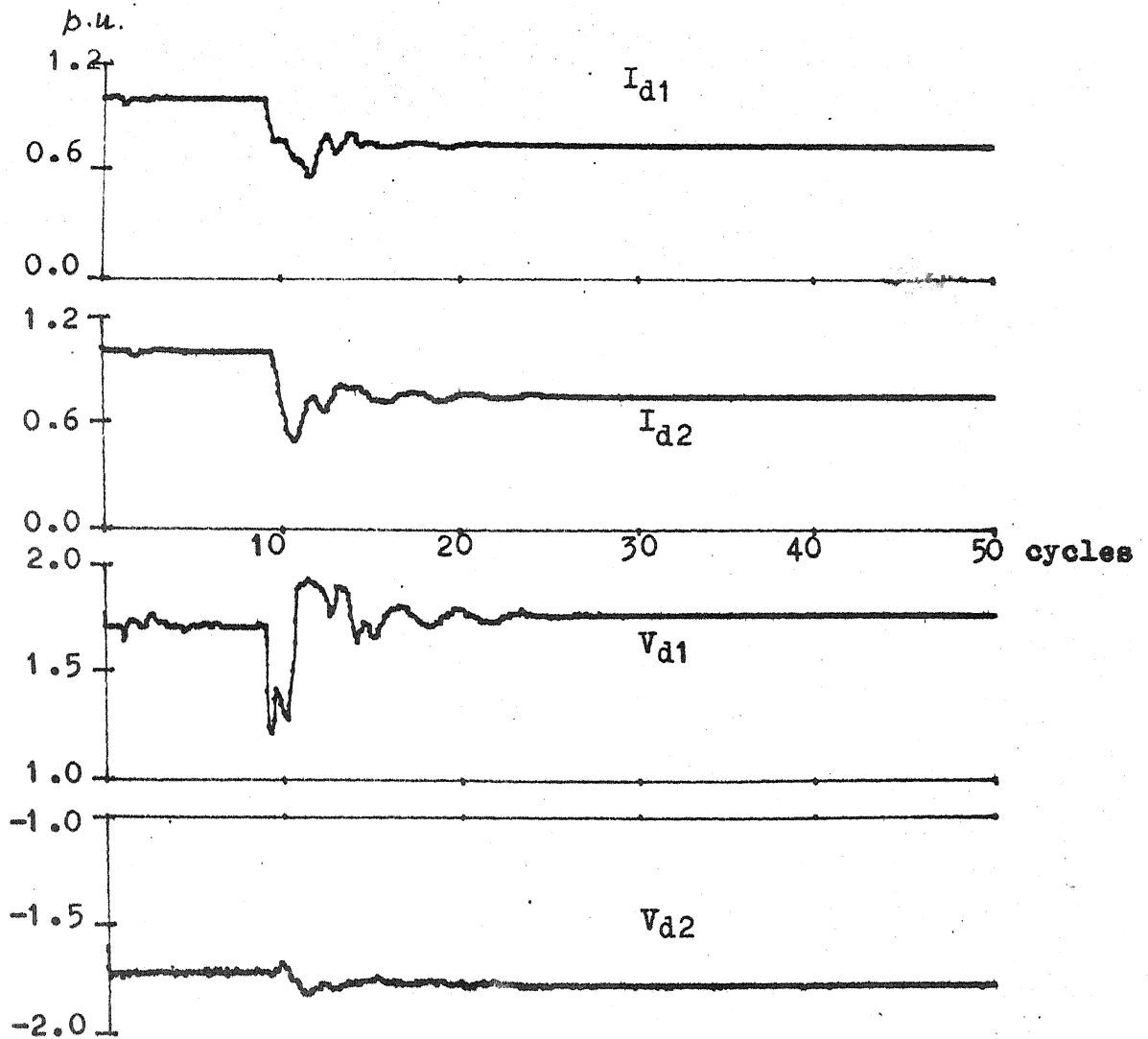
I_{ref1} : 1.0 to 0.75

I_{ref2} : 0.8 to 0.55

IPC at inverter; EPC at rectifier

SCR = 15.0

Fig. 4.16 CASE B(1)



I_{ref1} : 1.0 to 0.75

I_{ref2} : 0.8 to 0.55

EPC at rectifier; IPC at inverter

SCR = 7.0

Fig. 4.17 CASE B(11)

program developed earlier is suitably changed to incorporate the ac system representation. Steady state and transient responses of single and two terminal system are presented respectively. The responses not only show the influence of ac systems and filters but also points out that dynamic performance of HVDC system connected to ac system of low SCR can be improved greatly by employing EPC at the rectifier alone.

CHAPTER 5

CONCLUSION

This thesis is mainly devoted to the development of a 12 pulse converter model for dynamic digital simulation of HVDC system to investigate the control system response. All the subsystems including the dc network, ac system with filters, converter and the control system have been represented in detail.

The converter is represented by an equivalent circuit of a variable voltage source behind a variable impedance. Both these quantities are functions of the valve conduction pattern. This equivalent circuit is derived based on graph theoretic analysis. The model facilitates simulation of all possible modes of converter operations having continuous dc link current. The converter model is general enough to handle non-ideal valve characteristics and unsymmetrical source impedances.

The computer program developed incorporating the proposed converter model is modular in structure. As a result, it increases flexibility in the representation of individual subsystems.

The digital simulation was carried out on DEC 1090 system and to simulate one cycle of ac waveform the program takes 4 to 12 seconds of CPU time depending on the system details. This time can be further reduced by program optimization. Due to lack of standard test data, the results obtained in the thesis could not be compared with the results obtained from other methods of simulation.

Conclusions drawn from the test simulation results obtained in Chapters 3 and 4 are as follows :

1. EPC is more effective than IPC particularly when operating in a system without ac filters or when the converters are connected to a weak ac system.
2. The system performance is critically dependent on the controller configuration and parameters.

The major thrust in this thesis was on the development of the necessary software for the dynamic digital simulation of 12 pulse converters. However, the following aspects have not been taken into account :

1. Detailed representation of synchronous generator and transformer with their associated magnetic non-linearities.

2. The study of the performance of static var compensation in the integrated ac/dc power system.
3. Program optimization using more efficient numerical technique.

REFERENCES

1. G. Kron, 'Tensor for Circuits', Dover, 1959.
2. N.G. Hingorani, R.H. Kitchin and J.L. Hay, 'Dynamic simulation of HVDC power transmission systems on digital computer - Generalised mesh analysis approach', IEEE Transactions on Power Apparatus and Systems, vol. 87, April 1968, pp. 989-996.
3. J.L. Hay and N.G. Hingorani, 'Dynamic simulation of multiconverter HVDC system by digital computer, Part I: Mathematical Model and Part II : Computer Program', IEEE Trans. on Power Apparatus and Systems, vol. 89, February 1970, pp 218-228.
4. S. Williams and I.R. Smith, 'Fast digital computation of 3-phase thyristor bridge circuits', Proceedings of IEE, vol. 120, pp 791-795, July 1973.
5. N. Vovus, G. Galanos and G. Giannakopoulos, 'A mathematical model for dynamic simulation of HVDC systems', IEEE Transactions on Power Apparatus and Systems, vol. 102, No.6, June 1983, pp. 1755-1763.
6. K.R. Padiyar and Sachchidanand, 'Digital simulation of multiterminal HVDC system using a novel converter model', IEEE Transactions on Power Apparatus and Systems, vol. 102, No.6, June 1983, pp. 1624-1632.

7. A.M. El-Serafi and A. Shehata, 'Digital simulation of AC/DC systems in direct phase quantities', IEEE Transactions on Power Apparatus and Systems, vol. 95, March/April 1976, pp 731-736.
8. N.G. Hingorani, J.L. Hay and R.E. Crosbie, 'Dynamic simulation of HVDC systems on a digital computer', Proceedings of IEE, vol. 113, May 1966, pp 793-802.
9. J.S.C. Htsui and W. Shepherd, 'Method of digital computation of thyristor circuits', Proceedings of IEE, vol. 118, August 1971, pp 990-998.
10. J.G. Kassakian, 'Simulating Power Electronic systems - A new approach', Proceedings of the IEEE, vol. 67, No.10, October 1979, pp 1428-1439.
11. J. Reeve and J. Carr, 'Dynamic digital simulation of HVDC converter control and its application to system studies', IEEE Transactions on Power Apparatus and Systems, vol. 93, January/February 1974, pp. 296-302.
12. J. Reeve and J.A. Baron, 'Harmonic interaction between HVDC converters and AC power systems', IEEE Transactions on Power Apparatus and Systems, vol. 90, November/December 1971, pp 2785-2791.
13. J. Reeve and T. Subbarao, 'Dynamic analysis of harmonic interaction between AC and DC power systems', IEEE Transactions on Power Apparatus and Systems, vol. 93, March 1974, pp 640-646.

14. N.G. Hingorani and M.F. Burberry, 'Simulation of AC system impedance in HVDC system studies', IEEE Transactions on Power Apparatus and Systems, vol. 89, March 1970, pp 640-646.
15. N.G. Hingorani and P. Chadwick, 'A new constant extinction angle control for AC/DC/AC static converter', IEEE Transactions on Power Apparatus and Systems, vol. 87, March 1968, pp 866-872.
16. J.D. Ainsworth, 'The phase locked oscillator - A new control system for controlled static converters', IEEE Transactions on Power Apparatus and Systems, vol. 87, March 1968, pp 859-865.
17. A. Ekstrom and G. Liss, 'A refined HVDC control system', IEEE Transactions on Power Apparatus and Systems, vol. 89, May/June 1970, pp 723-732.

APPENDIX A

The dc base quantities are chosen as

DC base voltage is ideal no-load dc voltage of a bridge = 100 KV

DC base current = 1 KA

DC base impedance = 100 Ohms

The system parameters are adapted from reference [1].

Two terminal system

Rated Power of the DC link = 240 MW

AC system frequency = 50 cycles

Bridge transformer :

Resistance $R_{c1} = R_{c2} = 0.5$ ohms

Commutating Reactance $X_{c1} = X_{c2} = 6.283$ Ohms

Smoothing Reactor :

Resistance $R_{d1} = R_{d2} = 0.1$ Ohms

Reactance $X_{d1} = X_{d2} = 314.159$ Ohms

Transmission line :

Total resistance = 8.64 Ohms

Total Inductance = 0.50148 H

Total Capacitance = 54.1645 μ F

Controllers :

- a) Individual phase control

$$K_1 = K_2 = 2070 \text{ Ohms units}$$

$$T_{c1} = T_{c2} = 0.1 \text{ seconds}$$

- b) Equidistant phase control

$$K_1 = 0.001 \text{ rad/amp-sec.}$$

$$T_1/T_2 = 2.0, \quad T_2 = 0.0033 \text{ seconds}$$

RMS AC voltages (L-N) :

$$E_1 = 42.78 \text{ KV}, \quad E_2 = 38.51 \text{ KV}$$

Valve turn off time = 3°

Operating Conditions :

A. $I_{d1} = I_{d2} = 1000 \text{ Amps.}$

$$\alpha_{\min} = 5^\circ, \quad \gamma_c = 10^\circ$$

$$\alpha_1 = 26.22^\circ, \quad \alpha_2 = 148.39^\circ$$

B. $I_{d1} = I_{d2} = 1200 \text{ Amps}$

$$\alpha_{\min} = 5^\circ, \quad \gamma_c = 10^\circ$$

$$\alpha_1 = 26.77^\circ, \quad \alpha_2 = 145.59^\circ$$

Terminal 1 (rectifier) on constant current control and

Terminal 2 (inverter) on CEA controls.

APPENDIX B

From Fig. 4.1 it can be found out that three state variables are necessary and sufficient to describe the state of each phase (except filters) and the three generalised state equations for j th phase are

$$\dot{i}_{1j} = [-(-1)^j e_j - (-1)^{j+1} (i_{1j} - i_{2j}) R_s] / L_s \quad (\text{B.1})$$

$$\dot{i}_{2j} = [-(-1)^j (i_{1j} - i_{2j}) R_s - (-1)^{j+1} E_j] / L_s \quad (\text{B.2})$$

$$\dot{C}_j = [I_p - I_{Fj} + (-1)^j i_{1j}] / C_s \quad (\text{B.3})$$

where

$$I_p = I_A \quad \text{if} \quad j = 1$$

$$I_p = -(I_B + I_A) \quad \text{if} \quad j = 2$$

$$I_p = I_B \quad \text{if} \quad j = 3$$

$E_j \equiv$ instantaneous ideal source voltage of phase j ,
 $j = 1, 2, \text{ and } 3.$

$$I_{Fj} = \sum_{K=1}^n i_{tfj}^K + (i_{h fj} + (e_j - v_{nfj}) / R_{nf})$$

where i_{tfj}^K is the current through the K th tuned filter and $i_{h fj}$ is current through the high-pass filter.

The block marked 'F' in Fig. 4.1 represents a set of series tuned filters (5th, 7th, 11th and 13th) and a high pass second-order filter. A series tuned filter as shown in Fig. B.1 can be represented by two state equations as

$$\dot{i}_{tfj}^K = [e_j - v_{tfj}^K - R_{tf}^K i_{tfj}^K] / L_{tf}^K \quad (B.4)$$

$$\dot{v}_{tfj}^K = i_{tfj}^K / C_{tf}^K \quad (B.5)$$

while the state equations describing the high-pass filter shown in Fig. B.2 can be written as

$$\dot{i}_{hfj} = [e_j - v_{hfj}] / L_{hf} \quad (B.6)$$

$$\dot{v}_{hfj} = [i_{hfj} + (e_j - v_{hfj}) / R_{hf}] / C_{hf} \quad (B.7)$$

where C_{tf}^K , L_{tf}^K and R_{tf}^K are the capacitance, inductance and resistance of the Kth harmonic tuned filter, and C_{hf} , L_{hf} and R_{hf} are the capacitance, inductance and resistance of the high pass filter.

e_j 's, the converter ac bus voltages are the output of the system whereas I_A , I_B and E_j are the input.

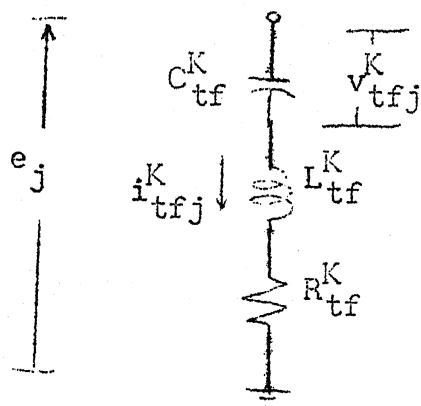


FIG. B.1: SERIES TUNED FILTER

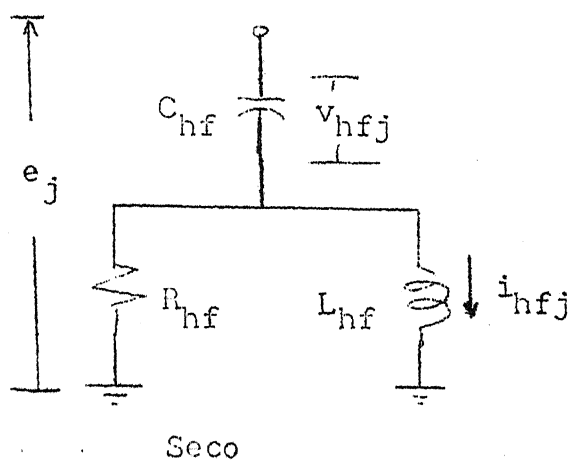


FIG. B.2: SECOND-ORDER HIGH PASS FILTER

APPENDIX C

All the ac system parameters are given with reference to the Fig. 4.1.

Single Terminal (Rectifier)

Transformer :

Tap $a = 1.0$

Resistance $R_c = 0.5$ Ohms

Reactance $X_c = 6.283$ Ohms

Converter :

Valve turn off time = 3°

AC Bus Voltage $e_j = 42.78$ KV
(L-N)

$\theta_j = 0.0^\circ$

DC current $I_d = 1000$ Amps

Constant Voltage Source $V_c = 166.449$ KV

$\alpha_{\min} = 7.0^\circ$, $\gamma_c = 10.0^\circ$

$\alpha_1 = 26.9^\circ$

Smoothing reactor

Resistance $R_d = 0.1$ Ohms

Reactance $X_d = 314.159$ Ohms

Controller :

a) Individual phase control

$K_1 = 2070$ Ohms

$T_c = 0.002$ seconds

b) Equidistant Pulse Control

$$K_1 = 0.001 \text{ rad/amp-sec}$$

$$T_1/T_2 = 2 ; \quad T_2 = 0.0033 \text{ seconds.}$$

Operating Condition :

A : With filters :

AC System :

Short circuit ratio SCR = 15

Impedance angle = 85°

Resistance $R_s = 4.16585 \text{ Ohms}$

Reactance :

Inductive $L_s = 0.74044 \text{ Ohms}$

Capacitive $C_s = 263.676 \text{ Ohms}$

Ideal ac source voltage

$$E_j = 43.88 \text{ KV}$$

$$\theta_j = 13.20948^\circ$$

B : Without filters

AC System :

Short circuit ratio SCR = 15

Impedance angle = 85°

Resistance $R = 4.3072 \text{ Ohms}$

Reactance :

Inductive $L_s = 0.76559 \text{ Ohms}$

Capacitive $C_s = 263.676 \text{ Ohms}$

Ideal ac source voltage

$$E_j = 44.67 \text{ KV}$$

$$\theta_j = 13.17981^\circ$$

Two terminal :

AC system is represented at Inverter only.

Only AC system and operating conditions are given below.

Other system parameters are same as given in Appendix B.

RMS ac source voltage (L-N) at rectifier

$$e_1 = 42.78 \text{ KV}$$

$$\theta_1 = 0.0^\circ$$

at inverter

$$e_2 = 38.51 \text{ KV}$$

$$\theta_2 = 0.0^\circ$$

DC current $I_{d1} = I_{d2} = 1.0 \text{ KV}$

$$\alpha_1 = 26.9^\circ, \quad \alpha_2 = 148.39^\circ$$

Operating conditions :

C : Short circuit ratio $\text{SCR} = 15$

Impedance angle $= 85^\circ$

Resistance $R_s = 3.04 \text{ Ohms}$

Reactance :

Inductive $L_s = 0.605 \text{ Ohms}$

Capacitive $C_s = 263.676 \text{ Ohms}$

Ideal AC source at inverter

$$E_j = 39.088 \text{ KV}$$

$$\theta_j = 7.83597^\circ$$

Transformer tap $a_1 = a_2 = 1.0$

D : Short circuit ratio $SCR = 7.0$

Impedance angle $= 85^\circ$

Resistance $R_s = 6.1859 \text{ Ohms}$

Reactance :

Inductive $L_s = 1.0995 \text{ Ohms}$

Capacitive $C_s = 263.676 \text{ Ohms}$

Ideal AC source at inverter

$E_j = 39.112 \text{ KV}$

$\theta_j = 6.004^\circ$

Transformer tap $a_1 = a_2 = 1.0$.

Filter Parameters

These parameters are taken from the reference [3] and used for all the test simulations.

Harmonic No.	Resistance Ohms	Inductance mH	Capacitance μF
5	1.11413	362.2	11.1346
7	0.801103	181.6	11.13748
11	0.504805	726.5	11.5102
13	0.4225	520.4	11.5331
H.P.	16.1428	3.0041	11.5791